SAPIENZA
UNIVERSITÀ DI ROMA

Echocardiography of the right heart in pulmonary arterial hypertension. Insights from the ULTRA RIGHT VALUE study

Facoltà di Farmacia e Medicina
Dipartimento di Chirurgia Generale e Specialistica Paride Stefanini
Corso di dottorato in Fisiopatologia ed Imaging Cardio-Toraco-Vascolare

Dott. Domenico Filomena

Relatore
Prof. Roberto Badagliacca

SUMMARY

ABSTRACT

Aims: In pulmonary arterial hypertension (PAH), outcomes are determined by right ventricular (RV) functional adaption to increased afterload. Echocardiography is readily available for bedside RV evaluation; however, it remains poorly implemented in guideline-directed clinical decision-making due to evidence quality concerns not meeting regulatory standards.

Methods and Results: This multicenter study gathered echocardiographic data with centralized reading from 401 patients with prevalent PAH. Clinical data—including World Health Organization (WHO) functional class (FC), 6-minute walk distance (6MWD), brain natriuretic peptide (BNP)/NT-pro-BNP, invasive hemodynamics, the European Society of Cardiology (ESC)/European Respiratory Society (ERS) guidelines-derived 4-strata score, and the United States REVEAL 2.0 score—were also collected. The primary outcome was a composite of all-cause mortality and heart failure hospitalizations. The secondary outcome was the maintenance or achievement of low-risk status according to ESC/ERS and REVEAL 2.0

at the latest follow-up.

Echocardiographic measurements revealed varying degrees of right heart dilation, assessed through right atrial and RV areas, along with altered indices of systolic function, including tricuspid annular plane systolic excursion (TAPSE), fractional area change, 2D strain, and estimates of RV to pulmonary artery (PA) coupling, obtained by relating RV systolic function metrics to systolic PA pressure (sPAP). All measurements were feasible.

Right heart dimensions and function metrics, particularly the TAPSE/sPAP ratio, correlated with WHO functional class, 6-minute walk distance, BNP/NT-pro-BNP levels, invasive hemodynamics, and both ESC/ERS and REVEAL 2.0 scores. Echocardiographic assessments were significantly associated with the composite endpoint of mortality and heart failure hospitalization and were predictive of maintaining or achieving low-risk status at follow-up. Echocardiography provided additional discriminative power, enhancing both ESC/ERS and REVEAL 2.0 scores, especially when a key risk score variable was missing.

Conclusions: This quality-controlled data from a network of PAH referral centers validates the associations between echocardiographic and pulmonary hemodynamic parameters and offers strong evidence for the prognostic value of morphological and functional echocardiographic variables in PAH. Our findings support the integration of echocardiographic assessments into existing risk stratification models for PAH patients.

INTRODUCTION

Pulmonary arterial hypertension (PAH) is a rare dyspnea-fatigue syndrome caused by a progressive increase in pulmonary vascular resistance (PVR) and right ventricular (RV) failure *[1,2]*. In spite of extensive pulmonary vascular remodeling, lung function in these patients is preserved and exercise limitation is determined by the cardiovascular system *[3]*. Evidence has been accumulated over the last decades that symptoms and outcome in PAH are mainly determined by RV function, yet there is no consensus on how to measure it in daily clinical practice *[1–5]*.

The right heart failure is heralded by increased dimensions and decreased systolic function in PAH [6]. The RV initially adapts to increased pulmonary artery pressure (PAP) by an enhanced contractility to preserve its coupling to the pulmonary circulation with no or minimal increase in its dimensions. When this "homeometric" systolic function response gets exhausted, the RV relies on a "heterometric" increase in dimensions to preserve flow output matching metabolic demand, at the price of increased

filling pressures and eventual systemic congestion [3–5]. Recent studies have shown that RV-pulmonary artery (PA) coupling in PAH has a functional reserve. The ratio of end-systolic to arterial elastance (E_{es}/E_a) must decrease from normal values of 1.5–2 to approximately 0.7 before significant changes in end-diastolic volume (EDV) occur and ejection fraction (EF) drops below 35%. However this timepoint is particularly relevant as this reduction in EF is associated with an increased risk of systemic congestion and poorer prognosis [7].

Gold standard measurements of the RV function require invasive conductance catheter technology, which is costly, time consuming, and not practical at the bedside *[8]*. Surrogate cardiac magnetic resonance imaging has been developed but this approach is still not widely available or sufficiently feasible in most PAH reference centers *[3–5]*. Therefore, PAH clinicians rely on simple daily routine echocardiographic examinations, mostly two-dimensional (2D) and complete their clinical assessment with brain natriuretic peptide (BNP) or N-terminal pro-BNP (NT-pro-BNP) determinations.

Risk stratification in PAH

Although specific treatments have improved survival in PAH patients [9], the disease remains progressive and carries a high mortality rate [10]. Therefore, risk assessment in PAH is crucial for both prognostication and guiding therapeutic decisions [11].

The 2015 European Society of Cardiology (ESC)/European Respiratory Society (ERS) Guidelines for the diagnosis and treatment of pulmonary hypertension introduced a multiparametric approach to risk assessment using a three-strata model, which classifies patients into low, intermediate, or high-risk categories [2]. This model incorporates variables such as clinical

evaluation, hemodynamics, imaging, exercise capacity, and NT-pro-BNP levels.

To further stratify the intermediate-risk group, a four-strata model was proposed, dividing patients into low, intermediate-low, intermediate-high, and high-risk categories, based on refined thresholds for WHO functional class, 6-minute walk distance (6MWD), and NT-pro-BNP [12,13]. This model has been evaluated in recent registry studies and is now recommended in the updated treatment algorithm for patients' follow-up, although the three-strata model is still used for initial risk assessment [1].

In addition to these models, other tools like the United States Registry to Evaluate Early and Long-Term Pulmonary Arterial Hypertension Disease Management (REVEAL) 2.0 risk score calculator have been developed [14]. This score incorporates several parameters, including age, sex, functional class, blood pressure, heart rate, six minute walking distance (6MWD), diffusing capacity of the lungs for carbon monoxide (DLCO), natriuretic peptides, right atrial pressure (RAP), pulmonary vascular resistance (PVR), and echocardiographic findings such as pericardial effusion.

Risk scores are increasingly recommended by current guidelines to support clinical decision-making for patients [1]. While these tools are widely used in clinical practice, certain limitations remain—particularly regarding the assessment of right ventricular (RV) function, which is still underemphasized, especially in patients evaluated using the ESC/ERS four-strata model. Moreover, when key variables are missing, the accuracy of risk scores diminishes, often resulting in risk overestimation that may lead to overtreatment [15].

Echocardiography in PAH risk prognostication

2D echocardiography provides a series of measurements of RV structure and function both at rest and during exercise *[16]*. While many of these measurements are included in current guidelines for the diagnosis and

treatment of PAH, they have not yet been integrated into the recommended risk scores *[1,2]*. Several of these measurements have been shown to be of prognostic relevance, but with methodological limitations preventing straightforward integration in current guidelines *[17]*. Establishing robust evidence for the utility of right heart echocardiography in detecting disease severity and assessing prognosis should be prioritized in PAH research [18,19].

Most recently, there has been report on improved REVEAL risk score by integration of echocardiographic assessments of RV dimensions, systolic function, tricuspid regurgitation (TR) severity and pericardial effusion *[20]*. However, as acknowledged by the authors, this was a retrospective sub-study, also limited by the subjective nature of the echocardiographic assessments. Consequently, there is still an unmet need of a multicentric prospective study with quantitative measurements and a centralized reading of the recordings, thus meeting currently required rigorous methodology *[21,22]*.

Therefore, the purpose of this study was to investigate the additive value of echocardiographic-derived right heart parameters, in improving patient's risk stratification.

Study Objective

Primary Objectives

The primary objective of the study was to assess the added value of right heart echocardiographic parameters, alongside clinical, functional, and hemodynamic variables, in predicting adverse events. Specifically, we aimed to evaluate the utility of echocardiography both in cases where one of the three key prognostic variables—WHO functional class, 6MWD, or

BNP/NT-proBNP—is missing for risk assessment and as a complement to a complete risk score assessment.

Secondary Objectives

The secondary objective of the study was to evaluate the correlation of the echocardiographic-derived right heart parameters with clinical and hemodynamic parameters of known prognostic relevance (i.e. NYHA/WHO functional class, 6MWD test, BNP/NT-pro-BNP level, cardiac index, RAP, and PRV), the ESC/ERS score, and the REVEAL 2.0 risk score.

METHODS

The ULTRAsound RIGHt venTricular eVALUation in pulmonary arterial hypertension (ULTRA RIGHT VALUE) study was an international multicenter observational prospective study enrolling prevalent patients with a diagnosis of PAH. The study employed a robust methodology and high-quality echocardiographic assessments, featuring centralized imaging interpretation.

Study Population

Inclusion Criteria

The inclusion criteria for the study were as follows:

1. Signed and dated Informed Consent Form (ICF);
2. Males and females aged ≥ 18 years;
3. Diagnosis of idiopathic, heritable, drug- and toxin-induced PAH, or PAH associated with connective tissue disease, human immunodeficiency virus, portopulmonary hypertension, or corrected congenital heart disease;
4. Confirmed diagnosis of precapillary pulmonary hypertension (PH) through right heart catheterization (RHC), in accordance with current guidelines at the time of evaluation;
5. Subjects willing and able to provide informed consent to participate in the study.

The hemodynamic definition of pre-capillary pulmonary hypertension was based on the criteria available at the time of enrollment: mean pulmonary artery pressure (mPAP) > 25 mmHg, pulmonary artery wedge pressure (PAWP) ≤15 mmHg, and PVR > 3 Wood Units until August 2022 and mPAP > 20 mmHg, PAWP ≤15 mmHg, and PVR > 2 Wood Units thereafter [1,2]. The diagnostic algorithm included also pulmonary function tests, ventilatory and perfusion lung scan, chest computed tomography, and echocardiography.

Exclusion Criteria

Patients were not considered eligible for enrollment into the study if they were diagnosed of one of the following groups of PH:

- Group 2: PH due to left heart disease
- Group 3: PH due to lung disease and/or hypoxia

- Group 4: Chronic Thromboembolic PH (CTEPH)
- Group 5: PH due to miscellaneous causes

Schedule Of Assessments

All subjects consecutively enrolled were assessed as follows:

- **Baseline Evaluation:** The subject's initial evaluation at the site.

- **Second Evaluation:** An evaluation conducted 6–12 months after the baseline, according to standard clinical practice.

- **Final Evaluation (End of Study):** An evaluation conducted 12 months after the second evaluation.

All the assessments were performed according to the common clinical practice, in accordance with the current clinical guidelines for PAH [1,2].

The study comprised the visits described below (all visits and assessments are listed in Table 1).

Table 1. Schedule of Study Assessments

	Name	**Baseline evaluation**	**Second Evaluation**	**Last evaluation[1]**
	Time	**DAY 0**	**6-12 months**	**1 months**
List of assessments				
Informed Consent		X		
Inclusion/Exclusion Criteria		X		
Demographic Data		X	X	X
Signs and Symptoms of PAH		X	X	X
Comorbidity		X	X	X
PAH-specific treatment		X	X	X

Concomitant therapies	X	X	X
6MWD	X	X	X
SBP	X	X	X
NYHA/WHO functional class	X	X	X
BNP or NT-proBNP	X	X	X
Right Heart Catheterization	X[2]	X[2]	X[2]
Echocardiography	X	X	X
ESC/ERS risk stratification score	X	X	X
REVEAL 2.0 risk score	X	X	X
Outcome assessment		X	X

6MWD= 6 Minute Walking Distance; BNP= Brain Natriuretic Protein; EOS= End Of Study; NYHA= New York Heart Association; NT-proBNP=N-terminal pro B-type Natriuretic Peptide; PAH= Pulmonary Arterial Hypertension; SBP= Systemic Blood Pressure; WHO= World Health Organization.

1 The EOS (end of study) was defined as the last evaluation performed in the study, and correspond with the last evaluation.

2 Right Heart Catheterization was performed according to the common clinical practice and was is not mandatory for the subject's enrollment.

Study Assessments and Procedures

All study assessments were performed by qualified study personnel (i.e. physician, nurse or specialist technical personnel), and were recorded at the time points indicated in the visit schedule (see section *Schedule of Assessments*).

Details of the study assessments are provided below.

Demographic Data

Demographic data collected include age, sex, weight, height, Body Mass Index.

Right Heart Catheterization

Right Heart Catheterization (RHC) was performed according to the common clinical practice and it was not mandatory for the subject's enrollment in the study. RHC was also not mandatory for patient's risk calculation according to the European and REVEAL 2.0 methods.

The nearest RHC to baseline, second and last evaluation was considered for the analysis (if performed no more than 3 months from the subject's evaluation and no change in specific therapy for PAH has occurred within that period).

Zero reference was levelled at mid chest in the supine position and cardiac output (CO) measured by thermodilution or Fick method (in case of severe tricuspid regurgitation, by measured oxygen consumption).

The following parameters were considered: heart rate (HR), systolic pulmonary arterial pressure (sPAP), diastolic PAP (dPAP), mPAP, PCWP, right atrial pressure (RAP), PVR, CO, cardiac index (CI), pulmonary arterial compliance (PA-C).

The PVR was calculated with the formula:

$$PVR = (mPAP – PCWP) / CO.$$

The CI was obtained dividing CO by body surface area. PA-C was

calculated with the formula:

PA-C=Stroke volume/systolic PAP – diastolic PAP.

Echocardiography

The echocardiographic exams were collected at each visit according to the common clinical practice. Standard M-mode, 2D, and Doppler images were acquired according to international guidelines [23].

Accreditation of Study Centers

Each center was required to perform an Echo Site Accreditation and send echo recordings to the ECL. The accreditation procedure ensured the repeatability of acquisition.

Echo Site Accreditation was achieved when the ECL verified that the center was proficient in the acquisition of image quality that would be suitable for qualitative and quantitative analysis by the ECL. If accreditation was not initially achieved, suggestions for improvements to standard echo were provided. The center could re-submit for accreditation evaluation when these improvements had been implemented and image quality had been improved.

Echocardiographic Core Laboratory

All echocardiographic imaging performed into this study were transferred electronically to the echocardiographic core laboratory located in Rome (Department of Clinical, Internal, Anesthesiological, and Cardiovascular Sciences - AOU Policlinico Umberto I, 'Sapienza' University of Rome, Italy). Echocardiographic images were automatically de-identified by the electronic software during the upload process, removing any identifiers from the Digital Imaging and Communication in Medicine (DICOM) header. The core laboratory evaluated all standard imaging recordings and interpreted the results according to standard guidelines [23–25].

Echocardiographic measurements

Measurements were provided through a vendor-independent software solution for cardiac ultrasound by Medis Medical Imaging. Image post-processing tools for advanced cardiac deformation analysis were used for the quantitative evaluation of imaging and for speckle tracking 2D strain assessment *[24,26]*. This new software allows clinicians to interact with the semi-automatically generated contours of the ventricles for manual editing and review purposes. The introduction of Rubber Banding in QStrain Echo Research Edition optimized the contour handling, including move-contour and smooth-contour functions.

The following parameters were measured and analyzed following US-European guidelines *[23,25]*: right atrial area (RA area), RV end-diastolic area (RVEDA), RV end-systolic area (RVESA), RV fractional area change % [RVFAC=(RVEDA - RVESA)/RVEDA x 100], tricuspid annular plane systolic excursion (TAPSE), left ventricular systolic and diastolic eccentricity

index (LVEIs and LVEId, respectively, defined as the ratio of the anterior–inferior and septal–posterolateral cavity dimensions in short axis, both in systole and diastole), left ventricular end-diastolic area, left ventricular end-systolic area, left ventricular ejection fraction (Simpson method), left atrial area, qualitative assessment of TR, inferior vena cava, estimation of sPAP from TR velocity, and the presence of pericardial effusion.

Pulsed Waved Tissue Doppler Imaging was used for the measurements of RV isovolumic contraction velocity (IVV), isovolumic acceleration (IVA) and peak systolic velocity (S').

To assess the segmental characteristics of the RV by speckle tracking analysis we adopted the 6-segment RV model. Peak systolic strain amplitude and time intervals from QRS onset to peak systolic strain were calculated for all the RV myocardial segments in the longitudinal direction. RV 2D global and RV free wall (FW) 2D basal-mid longitudinal strains (LS) were provided.

Time intervals were corrected for the heart rate according to the Bazett's formula *[27]*. To quantify RV dyssynchrony, we calculated the standard deviation (SD) of the times to peak-systolic strain for the 4 mid-basal RV segments corrected to the R-R interval between 2 QRS complexes to derive a so-called RV-SD4 index *[28,29]*.

Combined echocardiographic parameters to assess RV-PA coupling *[20]* were also reported as the ratio between RV systolic functional variables and sPAP: TAPSE/sPAP, RVFAC/sPAP, RV global LS/sPAP, RVFW basal-mid LS/sPAP. For patients with severe tricuspid regurgitation, where sPAP was not measurable, the invasive sPAP was used for the ratio calculation.

All reported measurements are the averages derived from three consecutive cardiac cycles.

Limits of normal were derived from the literature *[23,30]*.

ESC/ERS risk stratification score and REVEAL 2.0 risk score

Risk assessment relied on the ESC/ERS guidelines-derived 4-strata model *[31]*, which incorporates WHO functional class, 6MWD, and BNP/NT-pro-BNP, and on the REVEAL 2.0 score *[32]*, which incorporates etiology, age, sex, WHO FC, systolic blood pressure, heart rate, right atrial pressure (RAP), PVR, 6MWD, lung diffusing capacity for carbon monoxide, NT-pro-BNP, renal function, echocardiography, and previous hospitalization. Risk stratification was performed at each visit.

Outcomes

The primary outcome of this study was a composite of all-cause mortality and hospitalization for heart failure.

The secondary outcome was the maintenance or achievement of an ESC/ERS and REVEAL 2.0 low-risk status at the most recent evaluation.

Patients Management

The diagnostic work-up and management followed the 2015 ESC/ERS guidelines for patients enrolled up to the end of August 2022 *[2]* and the updated 2022 guidelines thereafter *[1]*. Treatments were prescribed

following contemporary guidelines available at the time of enrollment, according to clinician’s decision-making.

Statistical analysis

Continuous variables were expressed as mean ± standard deviation (SD) or median and interquartile range (IQR), and categorical variables were expressed as counts and percentages.

As all echocardiographic images were transferred using a web-based platform and centrally analyzed, we had no missing data for the present study.

Pearson's correlation (r) was used as a parametric measure of the strength and direction of association between two continuous variables. The Spearman’s correlation (ρ) was used as a nonparametric measure of the strength and direction of association between two variables measured on at least an ordinal scale. The Kendall's tau-b correlation coefficient (τb) was used as a nonparametric measure of the strength and direction of association that exists between two variables measured on an ordinal or continuous scale. Finally, the Somers' delta (Somers' d) was used as a nonparametric measure of the strength and direction of association between two categorical variables to distinguish between a dependent and independent variable.

Regression analysis was performed to assess the relations between RV systolic function parameters and PVR.

To compare the statistical significance of the difference between two correlation coefficients, we used the Fisher r-to-z transformation and calculated the p-value based on the resulting z-score.

Univariate Cox regression analysis, adjusted for age and PH duration, was performed to evaluate the association between morphological and functional echocardiographic parameters and the composite endpoint of mortality and heart failure hospitalization. Logistic regression analysis was conducted to assess the likelihood of maintaining or achieving a low-risk status according to the ESC/ERS and REVEAL 2.0 scoring systems, based on baseline echocardiographic variables.

The reciprocal transformations of odds ratios (ORs) and hazard ratios (HRs), represented as 1/OR and 1/HR, were also calculated to facilitate the comparison of ORs and HRs that are above and below 1. In this case, both presentations were provided.

The proportional-hazards assumption was tested using log-minus-log plots for categorical variables and the Schoenfeld residuals plots for continuous variables.

Cox proportional hazard (CPH) model was used to assess the impact of each isolated echocardiographic variable on the C-statistics in case of ESC/ERS and REVEAL 2.0 scores with missing variables. CPH was chosen due to its suitability for time-to-event analysis with few covariates. Each cross-validation round partitioned the n=401 patients into n=263 patients for training the risk predictor and n=138 patients as an independent cohort for testing. Of the 263 patients used for training, n=210 were used to fit the model to the data and n=56 were used to select the model hyperparameters.

The impact of echocardiography on top of the complete ESC/ERS and REVEAL 2.0 scores was analyzed by A.I. machine learning techniques, specifically, Random Survival Forest (RSF) model to learn the risk predictor [33]. RSF was chosen over CPH due to the higher number of variables involved.

Optional scaling (0-mean, 1-variance) and log-transform of variables was performed before feeding them to the models. Similarly, imputation was

used to replace missing values, chosing among 3 alternatives (average filling, nearest-neighbor-based, and regression-driven). Optimal preprocessing and modelling setup (e.g. whether to apply scaling, log-transform, type of imputation, model-specific hyperparameters such as number of survival trees) was tuned with randomized hyperparameter selection [34]. Predictive performances were assessed with average 3-fold cross validation C-statistics.

A.I. machine learning was also used to asses the impact of each variable, first by feature selection analysis with genetic algorithm and then confirmed with 100 rounds of permutation importance [35], which evaluates variable's influence by randomly shuffling its values and observing the change in C-statistics. Permutation invariance was preferred over built-in variable importance of RSF models for its ability to provide a more reliable, model-agnostic measure of relevance by directly assessing impact on C-statistics.

All statistical analyses were performed using open source package for R and Phyton.

Data Collection And Management

Data collection and completion of the Case Report Form

The investigator/delegate was responsible for ensuring the accuracy, completeness, and legibility of data reported. All source documents were completed in a neat, legible manner to ensure the accurate interpretation of data. Data were first documented in the subject’s source documents, and then transferred into electronic case report form (eCRF).

eCRF data were capture via electronic data capture. The investigator and clinical site staff were trained to enter and edit the data via a secure network, with secure access features (username, password). The investigator/delegate approved the data (i.e., confirm the accuracy of the data recorded) using an electronic signature (21 CFR Part 11).

All clinical information requested in this protocol was recorded by the investigator or his/her authorized staff in the eCRF in accordance with the study-specific data entry rules.

Periodically, a Clinical Research Associate (CRA) reviewed the accuracy, completeness, and timeliness of all the data entered in the eCRF.

Data protection

All clinical information was recorded, processed, handled, and stored without disclosing personal information of the subject so that it can be accurately reported, interpreted, and verified while the confidentiality of records and the personal data of the subject remains protected in accordance with the Regulation (EU) 2016/679 (General Data Protection Regulation).

Quality Control

A quality assurance and quality control system was implemented and maintained to ensure that the study was conducted, and data were generated, documented, and reported in compliance with the protocol, Good Clinical Practice (GCP), and applicable regulatory requirements. Quality control measures were applied at each stage of data handling to

ensure that all data were reliable and accurately processed.

Monitoring

Centralized monitoring was conducted to ensure proper study progression, safeguard the rights and well-being of participants, verify that the reported data were accurate, complete, and verifiable, and confirm that the study was conducted in accordance with the approved protocol, GCP, and all applicable regulatory requirements.

Ethical Consideration

Ethics and Good Clinical Practice

The study was conducted in accordance with Declaration of Helsinki, with the International Council on Harmonisation (ICH) Harmonised Tripartite Guideline for GCP (E6), and with the Commission Directive 2001/20/EC and 2005/28/EC, as well as with the valid national law of participating countries. The study was approved by the Institutional Review Board for Human Studies of each center (Protocol n. 638/18 for the Policlinico Umberto I - Sapienza University of Rome, coordinator center).

Informed consent was obtained prior to study participation. The subject and/or their legally authorized representative voluntarily confirmed participation after receiving a thorough explanation from the investigator and comprehensive written information about the study.

Study Organization

This study was sponsored by iPHNET, and was supported with an unrestricted grant by FERRER INTERNACIONAL SA for site management, site monitoring, and centralized imaging reading (in agreement with Italian Legislative Decree 43 of 17/12/2004, art. 2, subparagraph 6).

The U-RV protocol was designed and conducted under the guidance of a Steering Committee composed of clinicians with expertise in pulmonary hypertension and cardiovascular research. This committee was responsible for the protocol development, data collection tools, study oversight, and the review and publication of results. The Echocardiographic Core Laboratory (ECL) was comprised of a team of expert cardiologists specializing in echocardiographic imaging in PAH.

RESULTS

Patient population

Between January 2022 and December 2023, 401 patients with prevalent PAH were enrolled in the study by eight European referral centers for PAH. As shown in table 1, median age was 53 years (IQR 38-67) and the majority of the patients were female (275, 68%) with idiopathic PAH (244, 61%). Most of patients showed a pure PAH physiology, while 130 patients (32.4%) had at least one cardiometabolic comorbidity (table 1). WHO-FC was II or III in 357 (89%) patients. All patients enrolled were non-responders to acute vasodilator testing with nitric oxide at the time of diagnosis. Patients were evenly distributed across the ESC/ERS risk strata with the exception of a smaller group of high-risk patients (34, 8.5%). The distribution of REVEAL 2.0 risk scores was similar.

The median time from diagnosis to enrollment in the study was 34 months

(IQR 14-46).

One hundred sixty-nine patients (42.2%) were treated with double oral therapy (33.4%) or triple oral combination (8.8%), while 95 patients (23.5%) had received a parenteral prostacyclin.

Echocardiographic assessment was acquired 0±31 days (289 patients – 72%– within 24 hours) after right heart catheterization and before any change in therapies. B-mode 2D echocardiography and speckle tracking echocardiography were feasible in all patients. Pulse tissue Doppler imaging identified IVV in 70% of cases and IVA in 85% of cases. sPAP measurement was feasible in 98% of cases.

Baseline echocardiographic parameters showed variable dilation of the right heart and altered indices of systolic function or RV-PA coupling (table 2).

Right heart size and pulmonary hemodynamics

The sizes of the RV and RA were normally distributed, ranging from normal to severely increased, and were linearly related to all invasive pulmonary hemodynamic variables (table 3). Of note, only the TAPSE/sPAP ratio was always below the normal range of values.

Significant correlations were found among RV areas and invasive pulmonary hemodynamics, including RAP, mPAP, PVR and PA-C with the higher correlation found for RVESA (mPAP: $r = 0.37$, $p<0.001$; PVR: $r = 0.35$, $p<0.001$). We observed an increase of 0.42 cm^2 in RVEDA ($y = 24.2 + 0.42*x$, $p < 0.001$) and 0.52 cm^2 in RVESA ($y = 14.4 + 0.52*x$, $p < 0.001$) for every 1 Wood Unit (WU) increase in PVR. Figure 1 shows the positive correlation of RVESA with PVR (panel A) and the negative correlation with CI (panel B).

RA area was correlated with RV afterload parameters, including mPAP, PVR and PA-C, as well as with RV filling pressure, expressed as RAP, which showed the higher correlation (ρ =0.28, p<0.001) (figure 2). RA area was not correlated to CI (ρ = -0.09, p=ns).

As an indirect measure of RV dilation, LVEI in systole and diastole showed a non-normal distribution in the whole population. Both systolic and diastolic LVEI were positively correlated with RAP, mPAP and PVR, and negatively correlated with CI. LVEIs showed the highest correlation with mPAP and PVR (respectively, ρ = 0.42, p<0.001; ρ = 0.39, p<0.001).

Associations between right heart size estimates and WHO-FC, 6MWD, NT-pro-BNP, and risk scores

Patients with the most dilated RV and RA chambers had a more impaired clinical state and higher risk scores in both the ESC/ERS or the REVEAL 2.0 scoring systems.

RV and RA areas were positively correlated to WHO-FC and NT-proBNP, and negatively to the 6MWD. LVEIs and LVEId were positively correlated to WHO-FC and NT-proBNP. LVEId (not LVEIs) was negatively correlated to the 6MWD.

Area measurements of the RV and the RA for all patients at all ESC/ERS and REVEAL 2.0 scores are shown in Table 3 and figure 3. Both RV and RA areas were larger with increased risk, whether considering the ESC/ERS or the REVEAL 2.0 risk scores. RVESA showed slightly higher correlation coefficients compared with RVEDA and RA area (ESC/ERS score: τ_b = 0.30, p<0.001; REVEAL 2.0 score: τ_b = 0.31, p<0.001).

Adjustment of morphologic parameters for body surface area and tricuspid regurgitation

Normalization of ventricular and atrial areas for body surface area improved the correlation between RVEDA and RVESA, with PVR, PA-C and mPAP, without affecting others correlations (table 3).

When corrected for the severity of tricuspid regurgitation, the correlation between echocardiographic-derived right heart measurements and clinical variables, hemodynamics and risk scores did not improve meaningfully (supplementary table 1).

Right ventricular function correlation with pulmonary hemodynamics and risk scores

Both TAPSE and RVFAC were correlated with invasive pulmonary hemodynamics. The RVFAC showed a greater negative correlation with PVR and mPAP, and a positive correlation with PA-C, compared with TAPSE (table 3; figure 4). Conversely, TAPSE showed a better negative correlation with CI compared with RVFAC (respectively, $r= -0.41$, $p<0.001$, and $r= -0.34$, $p<0.001$), even when corrected for sPAP (respectively, $r= -0.44$, $p<0.001$, and $r= -0.36$, $p<0.001$). Differences in correlation coefficients between TAPSE and RVFAC for PVR, mPAP and PA-C decreased when variables were corrected for sPAP, further improving the correlation from moderate to strong (figure 5).

Similar correlation coefficients were observed between TAPSE and RVFAC for RAP distribution.

TAPSE and RVFAC were negatively correlated with WHO-FC and NT-proBNP, and positively correlated with the 6MWD. Both systolic function parameters were negatively associated with ESC/ERS and REVEAL 2.0 risk scores (figure 6). Correction of both TAPSE and RVFAC for sPAP did not improve substantially the correlation with clinical variables, except for the TAPSE/sPAP with the ESC/ERS and REVEAL 2.0 risk scores (figure 7).

IVV and IVA showed similar association with pulmonary hemodynamics, presenting positive correlation with RAP, PVR and mPAP, and negative correlation with PA-C. A higher correlation was observed between IVA and CI, compared with IVV (respectively, $r=0.31$, $p<0.001$; $r=0.14$, $p=0.04$). IVV was not correlated with clinical variables and risk scores. IVA was weakly correlated to clinical variables, as WHO-FC, 6MWD, NT-proBNP, and risk scores.

Both global RV LS and RVFW LS (excluding the apical segment) were correlated with invasive pulmonary hemodynamics. Both global RV LS and RVFW LS were positively correlated with RAP, PVR and mPAP, and negatively with PA-C and CI. Similar correlations characterized the association of both global RV LS and RVFW LS with WHO-FC, 6MWD, NT-proBNP, and risk scores. Of note, when the RV dilates, global RV LS is characterized by progressively reduced values compared with the RVFW LS of the basal and middle segments (figure 8).

Correction for sPAP did not improve the correlation between RV strain, whether global or free wall strain, and clinical variables and risk scores, but improved the correlation with all the invasive hemodynamic variables (table 3).

Of note, all RV systolic function variables showed similar clinical and hemodynamic correlations once corrected for sPAP, except for TAPSE/sPAP which presented the highest correlation with CI.

The relationship between RV systolic parameters—specifically RVFAC,

RV free wall strain, and TAPSE—and PVR had a flatter slope in severely dilated RVs compared to mildly dilated ones. In cases of mild RV dilation, RVFAC and RVFW LS showed a greater percentage decrease per unit increase in PVR compared to TAPSE, with reductions of 1.1%, 0.69%, and 0.46% per 1 PVR WU, respectively ($p<0.01$) (Figure 9).

Finally, when adjusted for the severity of tricuspid regurgitation, the correlation between echocardiographic-derived RV systolic function measurements and clinical variables, hemodynamics and risk scores did not improve meaningfully (supplementary table 1).

Right intraventricular dyssynchrony, calculated as RV-SD4, showed a significant correlation with the invasive hemodynamic variables, except for the PA-C, the WHO FC, the NT-pro-BNP and the ESC/ERS and REVEAL 2.0 risk scores. RV-SD4 was negatively correlated with 6MWD and CI.

Tricuspid regurgitation and pericardial effusion

There was a positive correlation between the severity of the disease expressed by the ESC/ERS and the REVEAL 2.0 scores and the grade of tricuspid regurgitation (table 3). However, the correlation of tricuspid regurgitation with each relevant component of the scores, as WHO-FC, 6MWD, and NT-proBNP, was weak. A very weak correlation, albeit significant, also characterized the association between invasive pulmonary hemodynamic and tricuspid regurgitation grade.

A significant but weak correlation was found between pericardial effusion and all clinical and hemodynamic variables, including the association with risk scores, whether the ESC/ERS or the REVEAL 2.0.

Echocardiographic predictors of morbi-mortality and risk status

During follow-up, fifty-four (13.5%) patients were hospitalized for heart failure (44, 11.0%) or died (10, 2.5%) after a median of 177 days (IQR 126–241). The univariate Cox regression analysis, adjusted for age and PH duration, revealed significant associations between various echocardiographic parameters and the composite endpoint of all-cause mortality and hospitalization for heart failure. Figure 10 illustrates the HRs for direct and combined echocardiographic variables along with their corresponding 95% confidence intervals. In the univariate Cox analysis, increased right heart dimensions and reduced LV dimensions were significantly associated with the primary outcome. Notably, a decrease in LVESA showed the strongest association, indicating a 22% increase in risk per 1 cm^2 decrease. Additionally, markers of reduced RV function, such as decreased TAPSE, RVFAC, RV deformation by strain analysis, and altered RV-PA coupling indices, were associated to a higher risk. Among these measures, RVFAC/sPAP, TAPSE/sPAP, RV global LS/sPAP, and RVFW basal-mid LS/sPAP exhibited the strongest associations with the outcome, showing increases in risk of 1.41 (1/0.71), 1.92 (1/0.52), 2.09, and 1.88-fold, respectively, per 0.1-unit decrease.

Figures 11 and 12 shows the likelihood of maintaining or achieving a low-risk status, according to the ESC/ERS and REVEAL 2.0 scoring systems, based on echocardiographic variables at baseline. For both risk scores, more dilated right heart chambers and higher indices of LV compression were associated with lower odds of achieving or maintaining a low-risk status. Notably, LVEId exhibited the strongest association, showing a 23% reduction in the probability of a low-risk score by REVEAL 2.0 and an 11% reduction by ESC/ERS for each 0.1-unit increase. The presence of pericardial effusion was associated with a 63% reduction in the odds of achieving or maintaining a low-risk status as measured by the ESC/ERS score, and a 69% reduction in the odds according to the REVEAL 2.0 score.

Similarly, higher RV functional parameters were associated with increased odds of achieving or maintaining a low-risk status, as assessed by both the ESC/ERS score and the REVEAL 2.0. Specifically, indices of RV-PA coupling—such as RVFAC/sPAP, TAPSE/sPAP, RV global LS/sPAP, and RVFW basal-mid LS/sPAP—showed the strongest associations, with fold increases in the odds of achieving or maintaining a low-risk status by the ESC/ERS score of 1.13, 1.25, 1.28 (1/0.78), and 1.25 (0.80), respectively, for each 0.1-unit increase. Similar results were also observed for the REVEAL 2.0 score.

Of note, a greater number of echocardiographic variables significantly associated with a REVEAL score below 6 for a low-risk definition, compared with a cut-value of 7 (supplementary table 2).

Echocardiographic value for risk tools with missing variables

We examined the accuracy of the ESC/ERS and the REVEAL 2.0 risk scores in case of missing variables, using the c-index (figure 13 and 14).

Missing one of the variables having higher prognostic value, as the WHO FC, the 6MWD and the BNP/NT-proBNP, the ESC/ERS risk tool was associated with significant reduction in discrimination compared with the complete score, respectively, c-index from 0.73 to 0.66, 0.69, 0.69. Similar results, but less pronounced, were observed considering missing WHO FC and 6MWD data in the REVEAL 2.0, respectively, c-index from 0.74 to 0.71 and 0.69, while missing BNP/NT-proBNP did not affect the discrimination capacity significantly (c-index 0.73).

We next used the Cox proportional hazard model to assess the impact of each isolated echocardiographic variable on the c-index in case of ESC/ERS and REVEAL 2.0 scores when one of the three major prognostic variables was missing. Cross-validation training and testing in an independent cohort resulted in improved risk discrimination of the ESC/ERS

score for the majority of the echocardiographic variables considered, with improved c-index ranging from 0.69 to 0.78 (figure 13). Similarly, risk discrimination improved for the REVEAL 2.0, with c-index ranging from 0.74 to 0.78 (figure 14). The echocardiographic variables able to increase the c-index in all missing data scenarios and for both scores, were LVESA, LVEIs and LVEId, RVFAC, RVFAC/sPAP, TAPSE, TAPSE/sPAP, TDI RV S', RVFW 2D mid-basal LS, RVFW 2D mid-basal LS/sPAP, RV 2D global LS, RV 2D global LS /sPAP, and TR grade.

Echocardiography on top of risk scores and impact of each variable through A.I. application

We analyzed whether the inclusion of echocardiography of the right heart was able to improve risk stratification assessed by the complete ESC/ERS and the REVEAL 2.0 scores. A Random Survival Forest model was used to learn the risk predictor. This approach was chosen over the Cox proportional hazard model due to the high number of variables involved. Predictive performances were assessed with average 3-fold cross validation c-index (see methods). The inclusion of all echocardiographic variables into the ESC/ERS and REVEAL 2.0 scores improved the c-index to 0.78 (95% C.I. 0.75-0.81) and 0.79 (95% C.I. 0.76-0.82), respectively.

To identify the impact of each echocardiographic variable among the spectrum of right heart remodeling in patients with prevalent PAH, we performed an innovative approach using first feature selection analysis with genetic algorithm, then confirmed by rounds of permutation importance, which evaluates variable's influence by randomly shuffling its values and observing the change in c-index (figure 15 and 16). This approach allowed to identify the relative importance of all echocardiographic variables used in the model, identifying a subset of parameters to use in clinical practice that would allow comparable performance with the complete model including all echocardiographic variables. For ESC/ERS risk score RVESA and RVFW

2D mid-basal LS/sPAP had the highest influence in c-index drop (> 0.01) when randomly shuffling their values. Additionally, for REVEAL 2.0 score we observed systolic dimensional metrics of the RV and LV (i.e. RVESA, LVESA, LV-EIs) together with corrected-variables for sPAP (i.e. RVFW 2D mid-basal LS/sPAP, RV 2 global LS/sPAP, TAPSE/sPAP) having the highest influence on the c-index. Compared with the ESC/ERS score, the REVEAL 2.0 showed a higher number of variable able to decrese the c-index by more than 0.01 when silencing their influence, including LVESA, LV-EIs, TDI RV IVA, RVFW 2D mid-basal LS, RV global LS/sPAP and TAPSE/sPAP.

DISCUSSION

The present results derive from a large multicenter collaboration with centralized core laboratory quality control. Right heart echocardiography was performed successfully across all eight participating centers, demonstrating excellent feasibility for nearly all relevant variables, with the exception of IVV and IVA measurements. Right heart dimension measurements and RV systolic function — particularly when combined with sPAP — correlated with hemodynamic severity and ESC/ERS and REVEAL risk scores, indirectly suggesting their prognostic relevance. Echocardiographic assessments significantly correlated with the composite endpoint of mortality and heart failure hospitalization and were predictive of maintaining or achieving a low-risk status. Notably, echocardiography added value to current risk stratification methods based on validated scores, especially when key variables were missing.

This is the first European experience of centralized echocardiography reading from multiple referral PAH centers with high quality data-imaging

collection, in accordance with imaging process standards by the U.S. Department of Health and Human Services and the Center for Biologics Evaluation and Research (U.S. Department of Health and Human Services Food and Drug Administration Center for Drug Evaluation and Research Center for Biologics Evaluation and Research) *[21]*.

Echocardiography in PAH generates a large number of variables, raising the question of which provide sufficient diagnostic and prognostic information in clinical practice. Redundant measurements may serve as internal controls, but are time-consuming and typically omitted in daily routine. The present study cannot answer the question of an ideal shortened list of the most relevant variables, as sequential correlation calculations only allow for a disqualification of non-significant ones, which were actually few. A hierarchy of correlation coefficients would be confused by a multiplicity problem, which can only be incompletely resolved with corrections for multiple comparisons. On the other hand, selecting independent predictors of risk scores by a uni/multivariable analysis could not be attempted in the present study because of the overwhelmingly large number of variables. Echocardiographic variables should be used in the framework of the previously discussed physiology of right heart structure and function adaptation to increased afterload in PAH *[3–5]*. In this respect, assessments of RV remodeling – mainly right atrial and ventricular areas, as well as the left ventricular eccentricity index, as highlighted in studies examining the RV response to drugs that effectively and significantly reduce PVR and improve prognosis *[36–38]* – are standard approach in daily clinical practice *[39]*.

Another important aspect is the evaluation of the coupling of RV systolic function to afterload *[5]*. The present results seem to support the TAPSE/sPAP ratio as the preferred variable compared with FAC/sPAP or strain/sPAP to assess the gold standard ratio of RV end-systolic elastance to pulmonary arterial elastance and predict outcome *[40]*.

Interestingly, the slope of the relation between RV systolic function

parameters and PVR was flatter for TAPSE in mildly dilated RVs compared with RVFAC and RVFW 2D strain, suggesting that the latter are more sensitive to detect disease progression-related changes in RV systolic function in the early stages of the disease.

Global RV strain was characterized by progressively reduced values compared with the RVFW strain of the basal and middle segments. This is probably related to technical issues affecting apical segment strain measurement. Indeed, high variability and reduced values characterize RV apical strain, even in normal subjects and especially in dilated RV chambers. This is supported by software-related technical issues *[41]*, as the measurements are dependent on cavity curvature and region of interest (ROI) width. Thus, because the apparent curvature and the ROI width/myocardial thickness discrepancy is highest in the apex, especially in dilated RV, measurements in apical RV segments are less reliable and characterized by high variability and reduced values *[28,29]*.The weak correlation of pericardial effusion and tricuspid regurgitation severity with RAP may be explained by the diuretic regimen optimized for prevalent patients. Greater correlations have been previously described for incident patients.

Echocardiography for risk prediction

In our study echocardiographic-derived morphological and functional parameters significantly correlated with the composite endpoint of mortality and hospitalization for heart failure, as shown by the Cox univariate analysis adjusted for age and pulmonary hypertension duration. Notably, while most of the right heart echocardiographic variables demonstrated a strong association with outcomes, RVEDA and pericardial effusion did not yield significant results.

The association between right heart echocardiographic parameters and clinical outcomes has been extensively demonstrated in prior research [42–46]. However, methodological limitations have prevented their inclusion in international recommendations and guidelines [1,2].

In our analysis, echocardiographic parameters indicating right heart enlargement, left ventricular compression, and reduced RV systolic function were associated with worse clinical outcomes. From a pathophysiological standpoint, echocardiography was able to capture aspects of heterometric RV adaptation, impaired ventricular-pulmonary artery (RV-PA) coupling, decreased RV systolic function, and elevated filling pressures—factors known to correlate with congestion, symptoms, reduced functional capacity, and adverse outcomes.

Additionally, we observed that baseline echocardiographic variables significantly influenced the likelihood of maintaining or achieving a low-risk status during follow-up, as defined by both the ESC/ERS and REVEAL 2.0 scoring systems. This finding is particularly relevant as maintaining or achieving a low-risk status should be a therapeutic goal, given that patients in this category have substantially better long-term survival than those in intermediate- or high-risk categories [1,47,48].

The issue of missing variables in prognostic scores is critical and can impact the clinical utility of risk prediction tools [1,15,49]. In our study, the absence of key prognostic variables, such as WHO functional class (FC), 6MWD, and BNP/NT-proBNP, significantly reduced the discrimination power of both the ESC/ERS and REVEAL scoring systems. For example, in our cohort, the c-index for the ESC/ERS risk tool decreased from 0.73 to 0.66 when one of these critical variables was missing, indicating a notable reduction in predictive capacity. Similarly, although the REVEAL 2.0 score showed less pronounced decreases, missing key variables still impacted its effectiveness.

These findings align with previous evidence, as shown by the COMPERA

registry, where the estimated risk increased for 20% to 44% of patients when one of the three most prognostic variables—BNP/NT-proBNP, 6MWD, and WHO FC—was missing [15]. Similar reductions in discrimination power were observed when applying the REVEAL Lite-2 score in clinical settings, particularly when BNP/NT-proBNP was missing, or when two variables were absent [49].

We demonstrated that integrating echocardiographic data could offer a potential solution for missing key variables. In particular, variables describing LV dimension and compression, RV dimension, and RV function (both in absolute values and indexed for afterload) improved the discriminative power of both risk scores in cases where variables were missing.

In our study we also explored the added value of echocardiography on top of current available risk score. The inclusion of echocardiographic parameters into the risk assessment models improved their discriminatory power. Importantly, this is the first European experience where A.I. algorithms have been used to prove the additional prognostic value of methodologically-sound collected echo variables on top of current risk tools. Using a Random Survival Forest model, we found that adding echocardiographic data enhanced the c-index for both the ESC/ERS and REVEAL 2.0 scores, reaching 0.78 and 0.79, respectively. Moreover, to further elucidate the contribution of individual echocardiographic variables, we employed a feature selection analysis combined with permutation importance. This innovative approach revealed that RVESA and RV 2D global LS/sPAP were among the most influential parameters in affecting the c-index. Notably, the REVEAL 2.0 score showed a greater sensitivity to changes in echocardiographic variables, as several parameters had a significant impact on the c-index when omitted.

These findings underscore the value of echocardiographic evaluation in refining risk assessment strategies for patients with PAH [37,50–52]. Previous studies have proposed enhancing PAH risk scores by

incorporating echocardiographic measurements of RV structure and function. In a retrospective series of 134 patients, only the LVED eccentricity index among standard echocardiographic assessments showed significant independent value when added to the REVEAL Lite 2 score, a validated simplified version of the REVEAL 2.0 score [53]. In a larger cohort of 2400 patients from the REVEAL registry, echocardiographic features, including the presence and severity of RV chamber enlargement, reduced RV systolic function, tricuspid regurgitation severity, and pericardial effusion, were used to derive a "REVEAL-ECHO score," which significantly improved the predictive capability of the REVEAL Lite 2 score as well [20]. However, right heart enlargement, severe tricuspid regurgitation, and pericardial effusion are typically late indicators of RV failure in PAH [3,54], and the REVEAL-ECHO score's assessment of systolic function was qualitative.

In this study, we provide high-quality data for the first time corroborating the evidence that echocardiography can offer additional discriminative power to currently available risk scores for predicting prognosis in PAH patients.

Limitations

This study has some limitations. First, the updated ESC/ERS guidelines in August 2022 introduced minor changes in patient management, leading to potential differences in treatment approaches before and after this date. Second, for a subset of patients, it was not possible to calculate sPAP via echocardiography; thus, invasive sPAP measurements were used to assess RV-PA coupling. Third, due to the limited number of patients with pericardial effusion (36 out of 283), a sensitivity analysis examining the correlation between pericardial effusion and pulmonary hemodynamics in patients with idiopathic, heritable, and toxin-induced PAH was not feasible. Additionally, the relatively low number of adverse events within the overall

cohort may limit the statistical power of our findings; a larger population with a greater number of events would be necessary to validate these results more robustly. Lastly, as most of the patients had idiopathic PAH or CTD-PAH, extending the present findings to other PAH subgroups warrants further investigation.

CONCLUSIONS

These findings confirm previously reported associations between echocardiographic and pulmonary hemodynamic parameters in smaller, primarily single-center studies of mixed-origin pulmonary hypertension populations and broaden our understanding of how varying stages of right heart impairment affect clinical status and risk assessment. This study provides robust evidence of the prognostic value of morphological and functional echocardiographic variables in PAH. Accordingly, our results support incorporating echocardiographic assessments into existing risk stratification models for patients with PAH, as these parameters can enhance risk prediction accuracy, informing clinical decisions and potentially improving patient outcomes. Particularly in cases of missing data, echocardiographic evaluations may enhance the completeness and precision of ESC/ERS or REVEAL 2.0 scores. Future research should continue investigating the role of echocardiography alongside established risk assessment tools to further validate and optimize these findings.

REFERENCES

1 Humbert M, Kovacs G, Hoeper MM, Badagliacca R, Berger RMF, Brida M, et al. 2022 ESC/ERS Guidelines for the diagnosis and treatment of pulmonary hypertension. Eur Heart J. 2022;43(38):3618–731.

2 Galiè N, Humbert M, Vachiery JL, Gibbs S, Lang I, Torbicki A, et al. 2015 ESC/ERS Guidelines for the diagnosis and treatment of pulmonary hypertension: The Joint Task Force for the Diagnosis and Treatment of Pulmonary Hypertension of the European Society of Cardiology (ESC) and the European Respiratory Society (ERS): Endorsed by: Association for European Paediatric and Congenital Cardiology (AEPC), International Society for Heart and Lung Transplantation (ISHLT). Eur Heart J. 2016 Jan;37(1):67–119.

3 Naeije R, Richter MJ, Rubin LJ. The physiological basis of pulmonary arterial hypertension. European Respiratory Journal. 2022 Jun;59(6). DOI: 10.1183/13993003.02334-2021

4 Noordegraaf AV, Chin KM, Haddad F, Hassoun PM, Hemnes AR, Hopkins SR, et al. Pathophysiology of the right ventricle and of the pulmonary circulation in pulmonary hypertension: an update. Eur Respir J. 2019 Jan;53(1). DOI: 10.1183/13993003.01900-2018

5 Tello K, Naeije R, De Man F, Guazzi M. Pathophysiology of the right ventricle in health and disease: an update. Cardiovasc Res. 2023 Aug;119(10):1891–904.

6 D'Alto M, Bossone E, Opotowsky AR, Ghio S, Rudski LG, Naeije R. Strengths and weaknesses of echocardiography for the diagnosis of pulmonary hypertension. Int J Cardiol. 2018 Jul;263:177–83.

7 Tello K, Dalmer A, Axmann J, Vanderpool R, Ghofrani HA, Naeije R, et al. Reserve of Right Ventricular-Arterial Coupling in the Setting of Chronic Overload. Circ Heart Fail. 2019 Jan;12(1):e005512.

8 Brener MI, Lurz P, Hausleiter J, Rodés-Cabau J, Fam N, Kodali SK, et al. Right Ventricular-Pulmonary Arterial Coupling and Afterload Reserve in Patients Undergoing Transcatheter Tricuspid Valve Repair. J Am Coll Cardiol. 2022 Feb;79(5):448–61.

9 Hoeper MM, McLaughlin V V., Dalaan AMA, Satoh T, Galiè N. Treatment of pulmonary hypertension. Lancet Respir Med. 2016 Apr;4(4):323–36.

10 Hoeper MM, Kramer T, Pan Z, Eichstaedt CA, Spiesshoefer J, Benjamin N, et al. Mortality in pulmonary arterial hypertension: prediction by the 2015 European pulmonary hypertension guidelines risk stratification model. Eur Respir J. 2017 Aug;50(2). DOI: 10.1183/13993003.00740-2017

11 Galiè N, Channick RN, Frantz RP, Grünig E, Jing ZC, Moiseeva O, et al. Risk stratification and medical therapy of pulmonary arterial hypertension. Eur Respir J. 2019 Jan;53(1). DOI: 10.1183/13993003.01889-2018

12 Hoeper MM, Pausch C, Olsson KM, Huscher D, Pittrow D, Grünig E, et al. COMPERA 2.0: a refined four-stratum risk assessment model

for pulmonary arterial hypertension. Eur Respir J. 2022 Jul;60(1). DOI: 10.1183/13993003.02311-2021

13 Boucly A, Weatherald J, Savale L, de Groote P, Cottin V, Prévot G, et al. External validation of a refined four-stratum risk assessment score from the French pulmonary hypertension registry. Eur Respir J. 2022 Jun;59(6). DOI: 10.1183/13993003.02419-2021

14 Benza RL, Gomberg-Maitland M, Elliott CG, Farber HW, Foreman AJ, Frost AE, et al. Predicting Survival in Patients With Pulmonary Arterial Hypertension: The REVEAL Risk Score Calculator 2.0 and Comparison With ESC/ERS-Based Risk Assessment Strategies. Chest. 2019 Aug;156(2):323–37.

15 Pausch C, Pittrow D, Hoeper MM, Huscher D. Performance of the ESC/ERS 4-strata risk stratification model for pulmonary arterial hypertension with missing variables. Eur Respir J. 2023 Nov;62(5). DOI: 10.1183/13993003.01023-2023

16 Gargani L, Pugliese NR, Biase N De, Mazzola M, Agoston G, Arcopinto M, et al. Exercise Stress Echocardiography of the Right Ventricle and Pulmonary Circulation. J Am Coll Cardiol. 2023 Nov;82(21):1973–85.

17 Naeije R. Assessment of right ventricular function in pulmonary hypertension. Curr Hypertens Rep. 2015 May;17(5). DOI: 10.1007/S11906-015-0546-0

18 Taylor RS, Elston J. The use of surrogate outcomes in model-based cost-effectiveness analyses: a survey of UK Health Technology Assessment reports. Health Technol Assess. 2009;13(8). DOI: 10.3310/HTA13080

19 Atkinson AJ, Colburn WA, DeGruttola VG, DeMets DL, Downing GJ, Hoth DF, et al. Biomarkers and surrogate endpoints: preferred definitions and conceptual framework. Clin Pharmacol Ther. 2001 Jan;69(3):89–95.

20 El-Kersh K, Zhao C, Elliott G, Farber HW, Gomberg-Maitland M, Selej M, et al. Derivation of a Risk Score (REVEAL-ECHO) Based on

Echocardiographic Parameters of Patients With Pulmonary Arterial Hypertension. Chest. 2023 May;163(5):1232–44.

21 The U.S. Department of Health and Human Services (Food and Drug Administration) and the Center for Biologics Evaluation and Research (U.S. Department of Health and Human Services Food and Drug Administration Center for Drug Evaluation and Research (CDER) Center for Biologics Evaluation and Research (CBER). The clinical trial imaging endpoint process standards. April 2018; https://www.fda.gov/Drugs/GuidanceComplianceRegulatoryInformation/Guidances/default.htm. [Internet]

22 Atkinson AJ, Colburn WA, DeGruttola VG, DeMets DL, Downing GJ, Hoth DF, et al. Biomarkers and surrogate endpoints: preferred definitions and conceptual framework. Clin Pharmacol Ther. 2001 Jan;69(3):89–95.

23 Rudski LG, Lai WW, Afilalo J, Hua L, Handschumacher MD, Chandrasekaran K, et al. Guidelines for the echocardiographic assessment of the right heart in adults: a report from the American Society of Echocardiography endorsed by the European Association of Echocardiography, a registered branch of the European Society of Cardiology, and the Canadian Society of Echocardiography. J Am Soc Echocardiogr. 2010 Jul;23(7):685–713.

24 Badano LP, Kolias TJ, Muraru D, Abraham TP, Aurigemma G, Edvardsen T, et al. Standardization of left atrial, right ventricular, and right atrial deformation imaging using two-dimensional speckle tracking echocardiography: a consensus document of the EACVI/ASE/Industry Task Force to standardize deformation imaging. Eur Heart J Cardiovasc Imaging. 2018 Jun;19(6):591–600.

25 Lang RM, Badano LP, Mor-Avi V, Afilalo J, Armstrong A, Ernande L, et al. Recommendations for Cardiac Chamber Quantification by Echocardiography in Adults: An Update from the American Society of Echocardiography and the European Association of Cardiovascular Imaging. Eur Heart J Cardiovasc Imaging. 2015 Mar;16(3):233–71.

26 Muraru D, Haugaa K, Donal E, Stankovic I, Voigt JU, Petersen SE, et al. Right ventricular longitudinal strain in the clinical routine: a state-of-the-art review. Eur Heart J Cardiovasc Imaging. 2022 Jun;23(7):898–912.

27 Bazett H. An analysis of the time-relations of electrocardiograms. Heart. 1920;7:353–70.

28 Badagliacca R, Reali M, Poscia R, Pezzuto B, Papa S, Mezzapesa M, et al. Right Intraventricular Dyssynchrony in Idiopathic, Heritable, and Anorexigen-Induced Pulmonary Arterial Hypertension: Clinical Impact and Reversibility. JACC Cardiovasc Imaging. 2015 Jun;8(6):642–52.

29 Badagliacca R, Poscia R, Pezzuto B, Papa S, Gambardella C, Francone M, et al. Right ventricular dyssynchrony in idiopathic pulmonary arterial hypertension: determinants and impact on pump function. J Heart Lung Transplant. 2015 Mar;34(3):381–9.

30 Ferrara F, Rudski LG, Vriz O, Gargani L, Afilalo J, D'Andrea A, et al. Physiologic correlates of tricuspid annular plane systolic excursion in 1168 healthy subjects. Int J Cardiol. 2016 Nov;223:736–43.

31 Hoeper MM, Pausch C, Olsson KM, Huscher D, Pittrow D, Grünig E, et al. COMPERA 2.0: a refined four-stratum risk assessment model for pulmonary arterial hypertension. Eur Respir J. 2022 Jul;60(1). DOI: 10.1183/13993003.02311-2021

32 Benza RL, Miller DP, Gomberg-Maitland M, Frantz RP, Foreman AJ, Coffey CS, et al. Predicting survival in pulmonary arterial hypertension: insights from the Registry to Evaluate Early and Long-Term Pulmonary Arterial Hypertension Disease Management (REVEAL). Circulation. 2010 Jul;122(2):164–72.

33 H W, G L. A Selective Review on Random Survival Forests for High Dimensional Data. Quant Biosci. 2017 Nov;36(2):85–96.

34 Bergstra J, Ca JB, Ca YB. Random Search for Hyper-Parameter Optimization Yoshua Bengio. Journal of Machine Learning Research. 2012 [cited 2024 Oct 28]. ;13:281–305.

35 Breiman L. Random forests. Mach Learn. 2001 Oct;45(1):5–32.

36 Badagliacca R, Raina A, Ghio S, D'Alto M, Confalonieri M, Correale M, et al. Influence of various therapeutic strategies on right ventricular morphology, function and hemodynamics in pulmonary arterial hypertension. J Heart Lung Transplant. 2018 Mar;37(3):365–75.

37 Badagliacca R, Papa S, Manzi G, Miotti C, Luongo F, Sciomer S, et al. Usefulness of Adding Echocardiography of the Right Heart to Risk-Assessment Scores in Prostanoid-Treated Pulmonary Arterial Hypertension. JACC Cardiovasc Imaging. 2020 Sep;13(9):2054–6.

38 D'Alto M, Badagliacca R, Argiento P, Romeo E, Farro A, Papa S, et al. Risk Reduction and Right Heart Reverse Remodeling by Upfront Triple Combination Therapy in Pulmonary Arterial Hypertension. Chest. 2020 Feb;157(2):376–83.

39 Rubin LJ, Naeije R. Sotatercept for pulmonary arterial hypertension: something old and something new. Eur Respir J. 2023 Jan;61(1). DOI: 10.1183/13993003.01972-2022

40 Tello K, Axmann J, Ghofrani HA, Naeije R, Narcin N, Rieth A, et al. Relevance of the TAPSE/PASP ratio in pulmonary arterial hypertension. Int J Cardiol. 2018 Sep;266:229–35.

41 NTNU-Trondhein Norwegian University of Science and Technology Strain rate imaging; www.ntnu.edu/isb/echocardiography. Dated 01/04/2024. [Internet]

42 Dong TX, Zhu Q, Wang ST, Wang YH, Li GY, Kong FX, et al. Diagnostic and prognostic value of echocardiography in pulmonary hypertension: an umbrella review of systematic reviews and meta-analyses. BMC Pulm Med. 2023 Dec;23(1):253.

43 Grapsa J, Pereira Nunes MC, Tan TC, Cabrita IZ, Coulter T, Smith BCF, et al. Echocardiographic and Hemodynamic Predictors of Survival in Precapillary Pulmonary Hypertension: Seven-Year Follow-Up. Circ Cardiovasc Imaging. 2015 Jun;8(6). DOI: 10.1161/CIRCIMAGING.114.002107

44 Bossone E, D'Andrea A, D'Alto M, Citro R, Argiento P, Ferrara F, et al. Echocardiography in pulmonary arterial hypertension: from diagnosis to prognosis. J Am Soc Echocardiogr. 2013 Jan;26(1):1–14.

45 Ghio S, Badagliacca R, Acquaro M, Filomena D, Recchioni T, Papa S, et al. Prognostic value of deep echocardiographic phenotyping in pulmonary arterial hypertension. ERJ Open Res. 2024 Jan;10(1). DOI: 10.1183/23120541.00587-2023

46 Shukla M, Park JH, Thomas JD, Delgado V, Bax JJ, Kane GC, et al. Prognostic Value of Right Ventricular Strain Using Speckle-Tracking Echocardiography in Pulmonary Hypertension: A Systematic Review and Meta-analysis. Can J Cardiol. 2018 Aug;34(8):1069–78.

47 Bouzina H, Rådegran G, Butler O, Hesselstrand R, Hjalmarsson C, Holl K, et al. Longitudinal changes in risk status in pulmonary arterial hypertension. ESC Heart Fail. 2021 Feb;8(1):680–90.

48 Badagliacca R, D'Alto M, Ghio S, Argiento P, Bellomo V, Brunetti ND, et al. Risk Reduction and Hemodynamics with Initial Combination Therapy in Pulmonary Arterial Hypertension. Am J Respir Crit Care Med. 2021 Feb;203(4):484–92.

49 Benza RL, Kanwar MK, Raina A, Scott J V., Zhao CL, Selej M, et al. Development and Validation of an Abridged Version of the REVEAL 2.0 Risk Score Calculator, REVEAL Lite 2, for Use in Patients With Pulmonary Arterial Hypertension. Chest. 2021 Jan;159(1):337–46.

50 Badagliacca R, Ghio S, D'Alto M, Ameri P, Correale M, Filomena D, et al. Relevance of Echocardiography-derived Phenotyping in Patients with Pulmonary Arterial Hypertension Treated with Initial Oral Combination Therapy: An Italian Pulmonary Hypertension Network (iPHNET) Study. Am J Respir Crit Care Med. 2024 May;210(3). DOI: 10.1164/RCCM.202402-0431LE

51 Ghio S, Mercurio V, Fortuni F, Forfia PR, Gall H, Ghofrani A, et al. A comprehensive echocardiographic method for risk stratification in

pulmonary arterial hypertension. Eur Respir J. 2020 May;56(3). DOI: 10.1183/13993003.00513-2020

52 Raymond RJ, Hinderliter AL, Willis IV PW, Ralph D, Caldwell EJ, Williams W, et al. Echocardiographic predictors of adverse outcomes in primary pulmonary hypertension. J Am Coll Cardiol. 2002 Apr;39(7):1214–9.

53 Sahay S, Bhatt J, Beshay S, Guha A, Nguyen DT, Graviss EA, et al. E-REVEAL Lite 2.0 scoring for early prediction of disease progression in pulmonary arterial hypertension. Pulm Circ. 2022 Jan;12(1). DOI: 10.1002/PUL2.12026

54 Sanz J, Sánchez-Quintana D, Bossone E, Bogaard HJ, Naeije R. Anatomy, Function, and Dysfunction of the Right Ventricle: JACC State-of-the-Art Review. J Am Coll Cardiol. 2019 Apr;73(12):1463–82.

TABLES

Table 1. Demographic, clinical and hemodynamic characteristics of the study population

Patients	**401**
Age, years	52±17
Female sex, (%)	275 (68%)
Weight, Kg	71±16
Height, cm	165±9
BSA, m^2	1.78 ±0.22
BMI, kg/m^2	26±5
Time from diagnosis, months	43±65
PAH classification, n (%)	
Idiopathic	244 (61)
Heritable	31 (8)
Drug/toxin-induced	8 (2)
CTD-SSc	66 (16)
CTD-non-SSc	27 (7)
HIV	8 (2)
Porto-pulmonary	11 (3)
CHD corrected	6 (1)
Comorbidities, n (%)	
Hypertension	56 (14.0)
Hypercholesterolemia	28 (7.0)
Coronary artery disease	17 (4.2)
Atrial fibrillation	19 (4.7)
Diabetes	10 (2.5)
N. of comorbidities, n (%)	
0	271 (67.6)
1	114 (28.4)
>1	16 (4.0)
WHO class, n (%)	
I	22 (5.5)
II	179 (44.6)
III	178 (44.4)
IV	22 (5.5)
6MWT, m	355±124
NT-proBNP, pg/ml	362 (140-1243)
Hemodynamics	
Heart rate, b/min	76±12
mPAP, mmHg	45±13
RAP, mmHg	7.3±4.2

CI, l/min/m2	2.6±0.8
PWP, mmHg	9.2±3.1
PVR, WU	8.8±5.0
Compliance, ml/mmHg	1.7±1.2
ESC/ERS score, n (%)	
Low	126 (31.4)
Intermediate-low	125 (31.2)
Intermediate-high	116 (28.9)
High	34 (8.5)
REVEAL 2.0 score, n (%)	
1-6	144 (35.9)
7-8	143 (35.7)
9-14	114 (28.4)
Specific therapy, n (%)	
ERA/ PDE5i monotherapy	94 (23.4)
Double oral combination	134 (33.4)
Triple oral	35 (8.8)
Mono oral + Epoprostenol i.v.	9 (2.1)
Mono oral + Treprostinil s.c.	6 (1.4)
Double oral + Epoprostenol i.v.	40 (10.0)
Double oral + Treprostinil s.c.	40 (10.0)
Others	44 (10.9)

Abbreviations: 6MWT: Six-Minute Walk Test, BMI: Body Mass Index, CHD: Congenital Heart Disease, CI: Cardiac Index, CTD-non-SSc: Connective Tissue Disease, non-Systemic Sclerosis, CTD-SSc: Connective Tissue Disease, Systemic Sclerosis, ERA: Endothelin Receptor Antagonist, ESC/ERS: European Society of Cardiology/European Respiratory Society, HIV: Human Immunodeficiency Virus, mPAP: mean Pulmonary Arterial Pressure, NT-proBNP: N-terminal pro b-type Natriuretic Peptide, PAH: Pulmonary Arterial Hypertension, PDE5i: Phosphodiesterase type 5 inhibitor, PVR: Pulmonary Vascular Resistance, PWP: Pulmonary Wedge Pressure, RAP: Right Atrial Pressure, REVEAL 2.0: Registry to Evaluate Early and Long-term PAH Disease Management, WHO: World Health Organization

Table 2. Echocardiographic characteristics of the study population

Echocardiographic parameter	Study Population	Reference Range
LVEDA, cm2	27.5±8.2	15.9-35.5 [a]
LVESA, cm2	12.2±4.7	8.1-21.3 [a]
LVEF, %	63.2±3.4	≥52 (M), ≥54(F) [b]
LV-EId, -	1.22 (1.06-1.41)	≤ 1.1 [c]
LV-EIs, -	1.27 (1.15-1.69)	≤ 1.1 [c]
LA area, cm2	18.3±5.4	≤ 20 [c]
RVEDA, cm2	27.5±8.2	≤ 25 [c]
RVESA, cm2	18.6±7.4	≤ 14 [c]
RVFAC, %	33.8±9.7	≥ 35 [c]
RVFAC/sPAP, %/mmHg	0.46 (0.33;0.69)	NA
TAPSE, mm	18.3±4.8	≥ 17 [b]
TAPSE/sPAP, mm/mmHg	0.25 (0.18;0.35)	≥ 0.7 [d]
TDI RV IVV, cm/s	7.9±3.1	NA
TDI RV IVA, cm/s^2	2.4 (1.8-3.3)	≥ 2.2 [c]
TDI RV S', cm/s	10.3±2.7	≥ 9.5 [b]
RV 2D global LS, %	-18.0±5.7	NA
RV global LS/sPAP, %/mmHg	-0.23 (-0.36;-0.16)	NA
RVFW 2D basal-mid LS, %	-21.0±6.9	NA
RVFW basal-mid LS/sPAP,%/mmHg	-0.32 (-0.47;-0.22)	NA
RV Dyssynchrony, ms	45±25	≤18 [e]
RA area, cm2	23.0±7.2	≤18 [c]
Tricuspid regurgitation, n (%)		
Mild	302 (75.3)	< Mild [c]
Moderate	90 (22.5)	
Severe	9 (2.2)	
IVC, mm	19.3+-5.4	≤21[c]
Pericardial effusion, %	54 (13.5)	Absent [c]

2D: two dimensional, EDA: end-diastolic area, EId: end-diastolic eccentricity index, EF: ejection fraction, EIs: end-systolic eccentricity index, ESA: end-systolic area, FAC: fractional area change, FW: free wall, IVC: inferior vena cava, IVA: isovolumic acceleration, IVV: isovolumic velocity, LA area: left atrial area, LS: longitudinal strain, LV: left ventricle, RA area: right atrial area, RV: right ventricle, S': systolic wave velocity, sPAP: systolic pulmonary artery pressure, TAPSE: tricuspid annular plane systolic excursion, TDI: tissue Doppler imaging.

a. Hausmann B, Hach H, Voigt B, Simon R. Echocardiography online quantification of left and right ventricular function by automatic boundary detection: reference values and reproducibility in healthy probands. Z Kardiol. 1994 Aug;83(8):556-61
b. Lang RM, Badano LP, Mor-Avi V, Afilalo J, Armstrong A, Ernande L, Flachskampf FA, Foster E, Goldstein SA, Kuznetsova T, Lancellotti P, Muraru D, Picard MH, Rietzschel ER, Rudski L, Spencer KT, Tsang W, Voigt JU. Recommendations for cardiac chamber quantification by echocardiography in adults: an update from the American Society of Echocardiography and the European Association of Cardiovascular Imaging. Eur Heart J Cardiovasc Imaging. 2015 Mar;16(3):233-70.
c. Derived from: Ferrara F, Rudski LG, Vriz O, Gargani L, Afilalo J, D'Andrea A, D'Alto M, Marra AM, Acri E, Stanziola AA, Ghio S, Cittadini A, Naeije R, Bossone E. Physiologic correlates of tricuspid annular plane systolic excursion in 1168 healthy subjects. Int J Cardiol. 2016 Nov 15;223:736-743
d. Badagliacca R, Reali M, Poscia R, Pezzuto B, Papa S, Mezzapesa M, Nocioni M, Valli G, Giannetta E, Sciomer S, Iacoboni C, Fedele F, Vizza CD. Right Intraventricular Dyssynchrony in Idiopathic, Heritable, and Anorexigen-Induced Pulmonary Arterial Hypertension: Clinical Impact and Reversibility. JACC Cardiovasc Imaging. 2015 Jun;8(6):642-52

Table 3. Correlation of echocardiographic variables with clinical and hemodynamic data.

	WHO	6MWD	NTproBNP	RAP	mPAP	PVR	PA-C	CI	ESC/ERS	REVEAL 2.0
LVEDA, cm^2	p<0.001 τ_b = -0.22	p<0.001 r = 0.20	p=0.003 r = -0.25	p=0.01 r = -0.15	p=0.007 r = -0.16	p<0.001 r = -0.30	p<0.001 r = 0.22	p<0.001 r = 0.25	p<0.001 τ_b = -0.27	p<0.001 τ_b = -0.26
LVEDA-i, cm^2/m^2	p<0.001 τ_b = -0.25	p=0.005 r = 0.17	p=0.02 r = -0.19	p=0.004 r = -0.17	p=ns r = -0.12	p=0.004 r = -0.17	p=0.01 r = 0.15	p<0.001 r = 0.23	p<0.001 τ_b = -0.29	p<0.001 τ_b = -0.27
LVESA, cm^2	p<0.001 τ_b = -0.17	p=0.002 r = 0.19	p=0.002 r = -0.26	p=0.02 r = -0.14	p<0.001 r = -0.20	p<0.001 r = -0.30	p<0.001 r = 0.26	p<0.001 r = 0.23	p<0.001 τ_b = -0.21	p<0.001 τ_b = -0.20
LVESA-i, cm^2/m^2	p<0.001 τ_b = -0.19	p=0.005 r = 0.17	p=0.01 r = -0.21	p=0.005 r = -0.17	p=0.005 r = -0.17	p<0.001 r = -0.21	p=0.001 r = 0.20	p<0.001 r = 0.22	p<0.001 τ_b = -0.21	p<0.001 τ_b = -0.20
LV-EId	p<0.001 τ_b = 0.19	p=0.01 ρ = -0.15	p<0.001 ρ = 0.31	p<0.001 ρ = 0.20	p<0.001 ρ = 0.32	p<0.001 ρ = 0.35	p<0.001 ρ = -0.23	p<0.001 ρ = -0.23	p<0.001 τ_b = 0.21	p<0.001 τ_b = 0.23
LV-EIs	p<0.001 τ_b = 0.16	p=ns ρ = -0.09	p=0.002 ρ = 0.26	p=0.002 ρ = 0.19	p<0.001 ρ = 0.42	p<0.001 ρ = 0.39	p<0.001 ρ = -0.29	p=0.01 ρ = -0.15	p<0.001 τ_b = 0.17	p<0.001 τ_b = 0.23
LA area, cm^2	p<0.001 τ_b = 0.20	p=ns r = 0.01	p=ns r = 0.04	p=ns r =-0.02	p=0.008 r = -0.16	p<0.001 r = -0.28	p=0.001 r = -0.19	p=0.003 r = -0.18	p<0.001 τ_b = 0.28	p<0.001 τ_b = 0.27

LA area-i, cm^2/m^2	p=ns τ_b = -0.06	p=ns r = 0.02	p=ns r = 0.04	p=ns r = -0.05	p=0.01 r = -0.14	p=0.002 r = -0.19	p=02 r = 0.14	p<0.001 r = 0.20	p=ns τ_b = -0.002	p=ns τ_b = -0.03
RA area, cm^2	p<0.001 τ_b = 0.20	p<0.001 r = -0.25	p<0.001 r = 0.41	p<0.001 r = 0.28	p<0.001 r = 0.24	p=0.01 r = 0.15	p=0.007 r = -0.16	p=ns r = -0.09	p<0.001 τ_b = 0.28	p<0.001 τ_b = 0.27
RA area-i, cm^2/m^2	p<0.001 τ_b = 0.19	p<0.001 r = -0.22	p<0.001 r = 0.45	p=0.003 r = 0.18	p=0.001 r = 0.19	p<0.001 r = 0.24	p=0.01 r = -0.15	p=ns r = -0.08	p<0.001 τ_b = 0.30	p<0.001 τ_b = 0.29
RVEDA, cm^2	p<0.001 τ_b = 0.22	p=0.006 r = -0.17	p<0.001 r = 0.39	p=0.002 r = 0.19	p<0.001 r = 0.30	p<0.001 r = 0.25	p=0.002 r = -0.12	p=0.003 r = -0.18	p<0.001 τ_b = 0.24	p<0.001 τ_b = 0.26
RVEDA-i, cm^2/m^2	p<0.001 τ_b = 0.22	p=0.02 r = -0.14	p<0.001 r = 0.41	p=0.04 r = 0.12	p<0.001 r = 0.34	p<0.001 r = 0.39	p=0.001 r = -0.19	p=0.002 r = -0.19	p<0.001 τ_b = 0.25	p<0.001 τ_b = 0.28
RVESA, cm^2	p<0.001 τ_b = 0.28	p<0.001 r = -0.23	p<0.001 r = 0.42	p<0.001 r = 0.23	p<0.001 r = 0.37	p<0.001 r = 0.35	p<0.001 r = -0.21	p<0.001 r = -0.26	p<0.001 τ_b = 0.30	p<0.001 τ_b = 0.31
RVESA-i, cm^2/m^2	p<0.001 τ_b = 0.28	p<0.001 r = -0.21	p<0.001 r = 0.44	p=0.003 r = 0.18	p<0.001 r = 0.40	p<0.001 r = 0.45	p<0.001 r = -0.27	p<0.001 r = -0.27	p<0.001 τ_b = 0.30	p<0.001 τ_b = 0.31
RVFAC, %	p<0.001 τ_b = -0.31	p<0.001 r = 0.30	p<0.001 r = -0.34	p<0.001 r = -0.24	p<0.001 r = -0.43	p<0.001 r = -0.44	p<0.001 r = 0.33	p<0.001 r = -0.34	p<0.001 τ_b = -0.32	p<0.001 τ_b = -0.31
RVFAC/sPAP, %/mmHg	p<0.001 τ_b = -0.29	p<0.001 ρ = 0.29	p<0.001 ρ = -0.40	p<0.001 ρ = -0.31	p<0.001 ρ = -0.78	p<0.001 ρ = -0.70	p<0.001 ρ = 0.71	p<0.001 ρ = 0.36	p<0.001 τ_b = -0.30	p<0.001 τ_b = -0.33
TAPSE,	p<0.001	p<0.001	p=0.001	p<0.001	p<0.001	p<0.001	p<0.001	p<0.001	p<0.001	p<0.001

mm	τ_b = -0.26	r = 0.31	r = -0.28	r = -0.28	r = -0.25	r = -0.38	r = 0.23	r = -0.41	τ_b = -0.29	τ_b = -0.27
TAPSE/sPAP, mm/mmHg	p<0.001 τ_b = -0.28	p<0.001 ρ = 0.31	p<0.001 ρ = -0.39	p<0.001 ρ = -0.36	p<0.001 ρ = -0.76	p<0.001 ρ = -0.73	p<0.001 ρ = 0.71	p<0.001 ρ = 0.44	p<0.001 τ_b = -0.30	p<0.001 τ_b = -0.35
pTDI IVA, m/s²	p=ns τ_b = -0.01	p=ns ρ = 0.004	p=ns ρ = -0.11	p=ns ρ = -0.11	p=0.005 ρ = -0.20	p=0.004 ρ = 0.20	p=0.003 ρ = 0.21	p=0.005 ρ = 0.20	p=ns τ_b = -0.03	p=ns τ_b = -0.02
pTDI IVV, cm/s	p=ns τ_b = -0.05	p=ns r = 0.08	p=ns r = -0.15	p=0.006 r = -0.19	p<0.001 r = -0.36	p<0.001 r = -0.32	p<0.001 r = 0.27	p=0.04 r = 0.14	p=ns τ_b = -0.06	p=ns τ_b = -0.08
pTDI s', cm/s	p=0.001 τ_b = -0.15	p=0.03 r = 0.15	p=0.005 r = -0.27	p=0.004 r = -0.19	p<0.001 r = -0.24	p<0.001 r = -0.36	p<0.001 r = 0.24	p<0.001 r = 0.31	p<0.001 τ_b = -0.17	p<0.001 τ_b = -0.16
RV 2D global LS, %	p<0.001 τ_b = 0.28	p<0.001 r = -0.29	p<0.001 r = 0.34	p<0.001 r = 0.23	p<0.001 r = 0.37	p<0.001 r = 0.40	p<0.001 r = -0.23	p<0.001 r = -0.32	p<0.001 τ_b = 0.31	p<0.001 τ_b = 0.31
RV 2 global LS/sPAP, %/mmHg	p<0.001 τ_b = 0.29	p<0.001 ρ = -0.28	p<0.001 ρ = 0.39	p<0.001 ρ = 0.30	p<0.001 ρ = 0.73	p<0.001 ρ = 0.69	p<0.001 ρ = -0.67	p<0.001 ρ = -0.38	p<0.001 τ_b = 0.31	p<0.001 τ_b = 0.34
RVFW 2D mid-basal LS, %	p<0.001 τ_b = 0.30	p<0.001 r = -0.29	p<0.001 r = 0.38	p<0.001 r = 0.21	p<0.001 r = 0.32	p<0.001 r = 0.34	p<0.001 r = -0.21	p<0.001 r = -0.27	p<0.001 τ_b = 0.32	p<0.001 τ_b = 0.31
RVFW 2D mid-basal	p<0.001 τ_b = 0.30	p<0.001 ρ = -0.29	p<0.001 ρ = 0.41	p<0.001 ρ = 0.32	p<0.001 ρ = 0.76	p<0.001 ρ = 0.69	p<0.001 ρ = -0.69	p<0.001 ρ = -0.36	p<0.001 τ_b = 0.31	p<0.001 τ_b = 0.31

LS/sPAP, %/mmHg										
RV dyssynchrony, ms	p=0.006 τ_b = 0.12	p=0.02 r = -0.14	p=0.002 r = 0.24	p=0.02 r = 0.14	p=0.03 r = 0.13	p=0.001 r = 0.20	ns r = -0.03	p=0.002 r = -0.19	p<0.001 τ_b = 0.14	p=0.002 τ_b = 0.13
Pericardial effusion	p=0.001 d = 0.24	p=0.002 τ_b = -0.16	p=ns τ_b = 0.11	p=0.03 τ_b = 0.11	p=0.01 τ_b = 0.12	p=0.01 τ_b = 0.13	p=0.03 τ_b = -0.11	p=0.03 τ_b = -0.10	p<0.001 d = 0.19	p<0.001 d = 0.33
Tricuspid reg, grade	p=0.002 d = 0.14	p<0.001 τ_b = -0.25	p<0.001 τ_b = -0.26	p=0.003 τ_b = 0.14	p=0.02 τ_b = 0.11	p<0.001 τ_b = 0.15	p=0.001 τ_b = -0.15	p=0.001 τ_b = -0.15	p<0.001 d = 0.25	p<0.001 d = 0.38

Abbreviations:

2D: two dimensional, 6MWD: Six-Minute Walk Distance, -i: indexed to body surface area, CI: Cardiac Index, ESC/ERS: European Society of Cardiology/European Respiratory Society, EDA: end-diastolic area, EId: end-diastolic eccentricity index, EF: ejection fraction, EIs: end-systolic eccentricity index, ESA: end-systolic area, FAC: fractional area change, FW: free wall, IVC: inferior vena cava, IVA: isovolumic acceleration, IVV: isovolumic velocity, LA area: left atrial area, LS: longitudinal strain, LV: left ventricle, NT-proBNP: N-terminal pro b-type Natriuretic Peptide, PA-C: Pulmonary Artery Compliance, PVR: Pulmonary Vascular Resistance, RA area: right atrial area, RAP: Right Atrial Pressure, REVEAL 2.0: Registry to Evaluate Early and Long-term PAH Disease Management 2.0, RV: right ventricle, S': systolic wave velocity, sPAP: systolic pulmonary artery pressure, TAPSE: tricuspid annular plane systolic excursion, TDI: tissue Doppler imaging, WHO: World Health Organization

r = Pearson's *r* correlation coefficient; τ_b = Kendall's tau-b correlation coefficient; ρ = Spearman rank-order correlation coefficient; d = Somers' delta correlation coefficient

FIGURES

Figure 1. Correlation of RVESA with PVR (panel A) and CI (panel B).

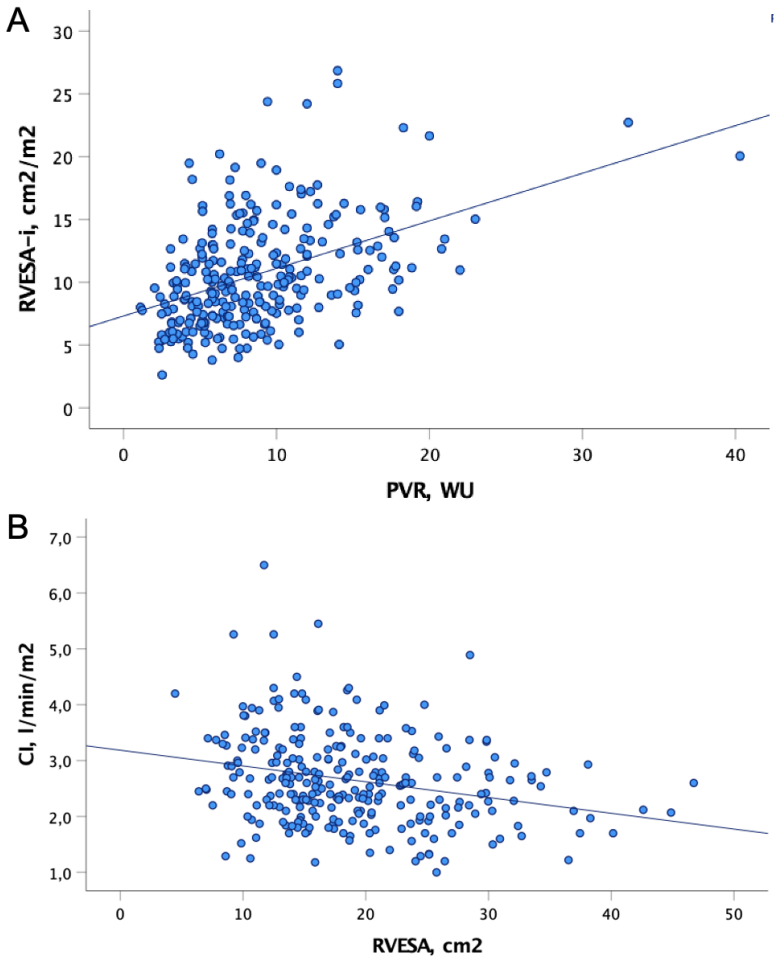

The plot shows a positive correlation between RVESA and PVR (r= 0.35, p<0.001)(panel A); a negative correlation with CI (r= -0.27, p<0.001)(panel B).

Abbreviations. RVESAi: right ventricular end-systolic area index; PVR: pulmonary vascular resistance; CI: cardiac index.

Figure 2. Correlation of RA area with RAP.

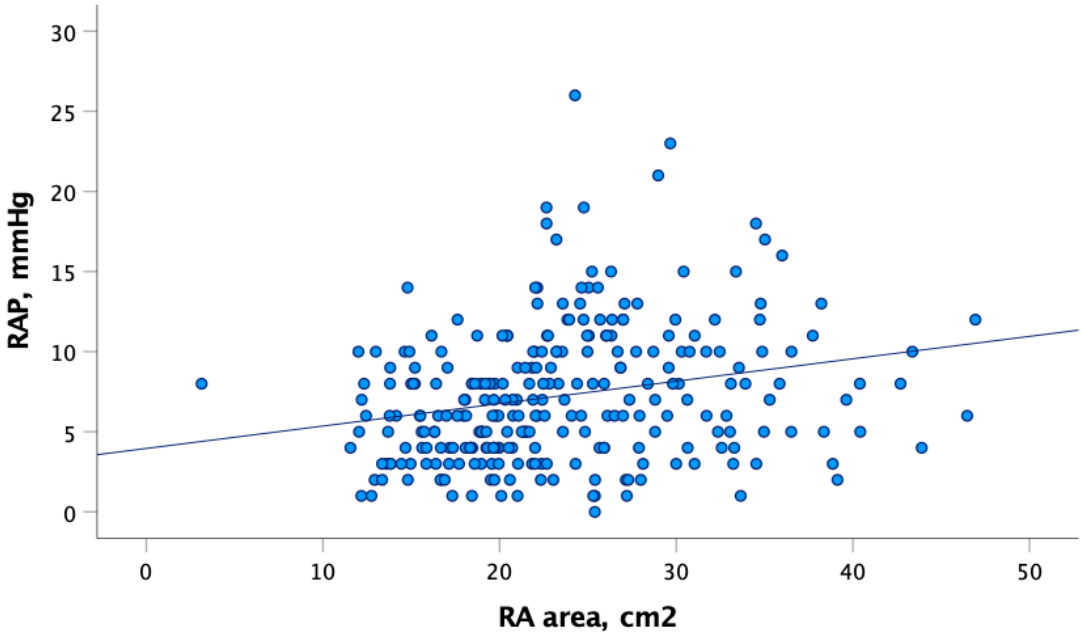

The plot shows significant positive correlation between RA pressure and area ($r = 0.28$, $p < 0.001$).

Abbreviations. RA: right atrium; RAP: right atrial pressure.

Figure 3. Box-and-whiskers plots showing the distribution of RVESA according to the ESC/ERS "4-strata" (panel A) and REVEAL 2.0 (panel B).

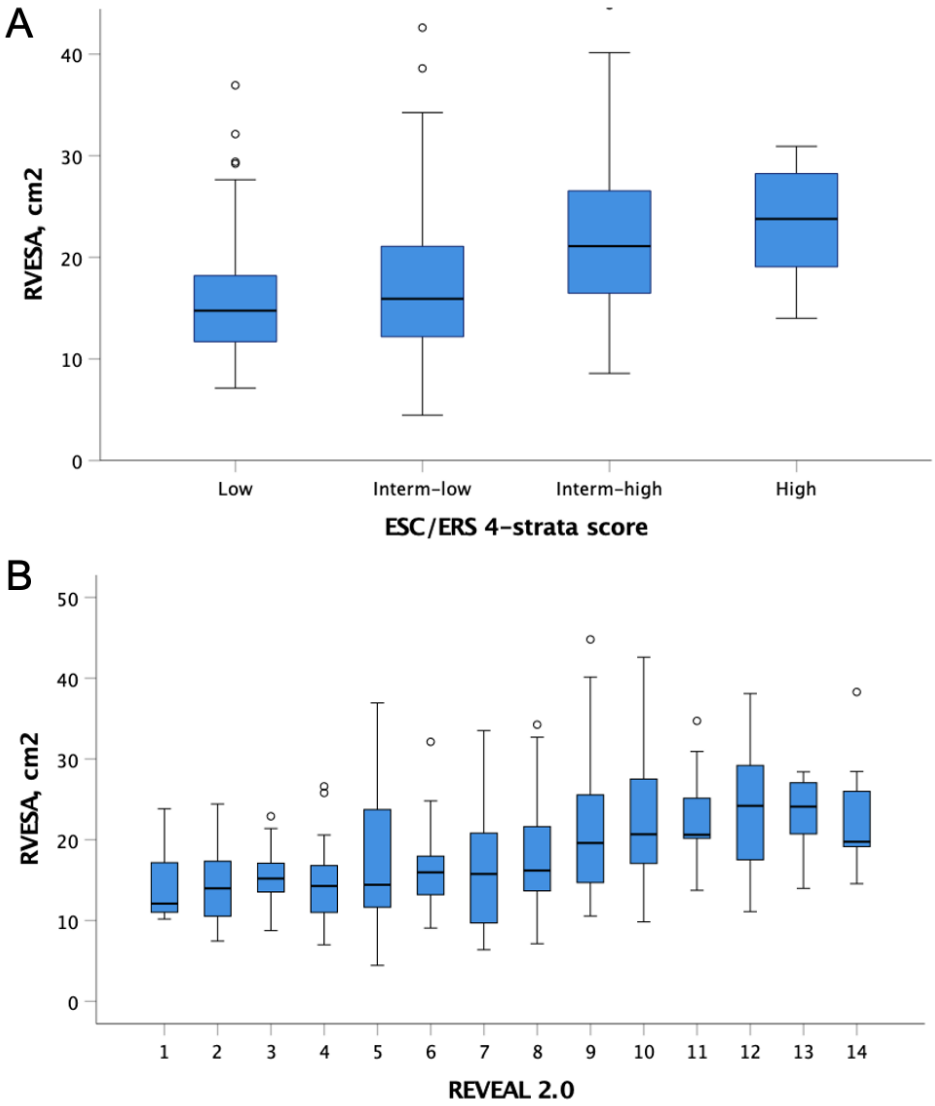

RVESA showed significant correlation with ESC/ERS and the REVEAL 2.0 risk score (ESC/ERS score: τ_b = 0.30, p<0.001; REVEAL 2.0 score: τ_b = 0.31, p<0.001).

Abbreviations. RVESA: right ventricular endsystolic area; ESC: European Society of Cardiology; REVEAL 2.0: United States Registry to Evaluate Early and Long-Term Pulmonary Arterial Hypertension Disease Management.

Figure 4. Correlation of PVR with RVFAC (panel A) and TAPSE (panel B).

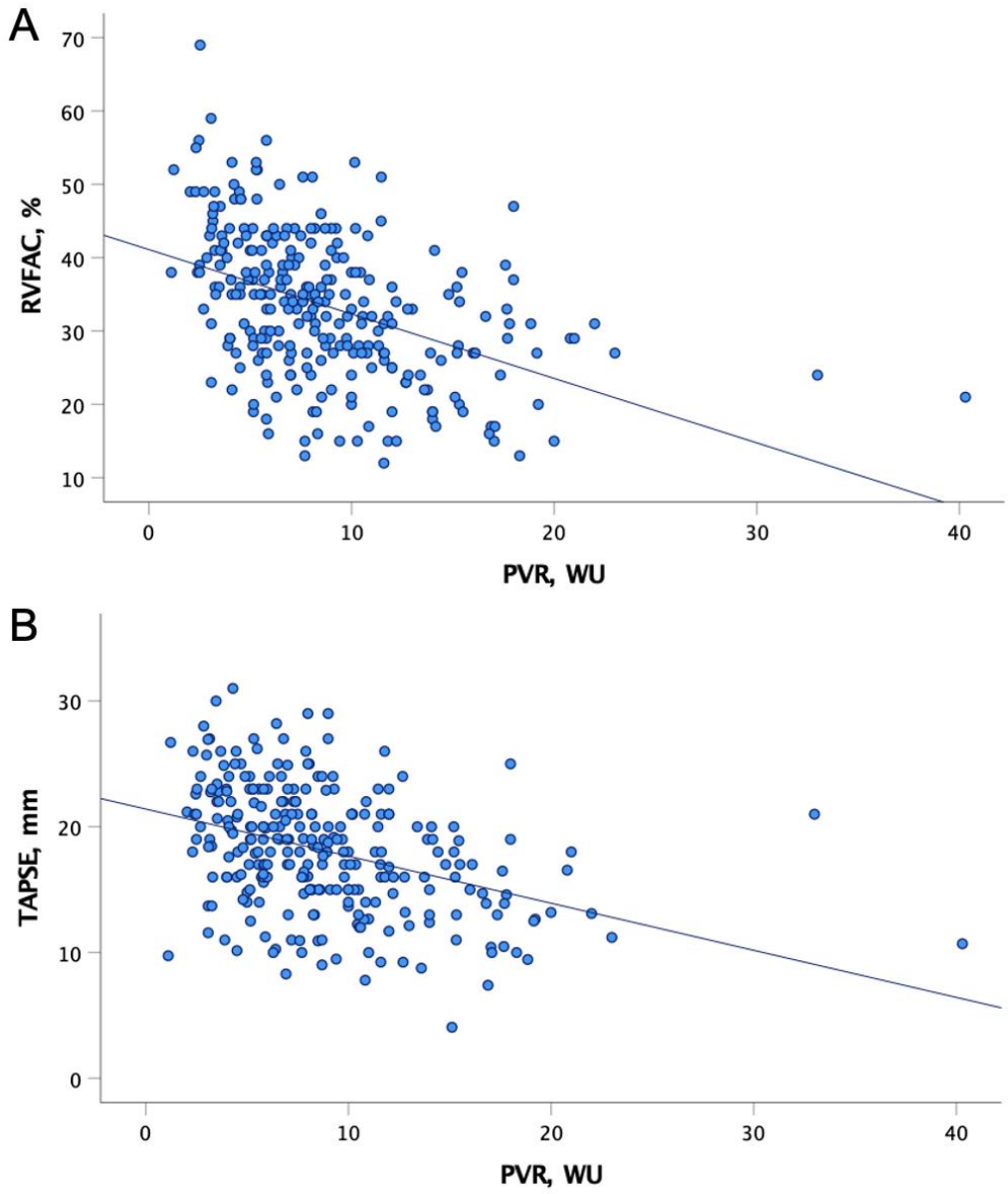

Both RVFAC and TAPSE showed a negative correlation with PVR, greater with RVFAC (respectively, r = -0.44, p<0.001; r = -0.30, p<0.001).

Abbreviations. RVFAC: right ventricular fraction area change; TAPSE: tricuspid annular plane systolic excursion; PVR: pulmonary vascular resistance, WU: wood unit.

Figure 5. Correlation of RVFAC/sPAP (panel A) and TAPSE/sPAP (panel B) with PVR.

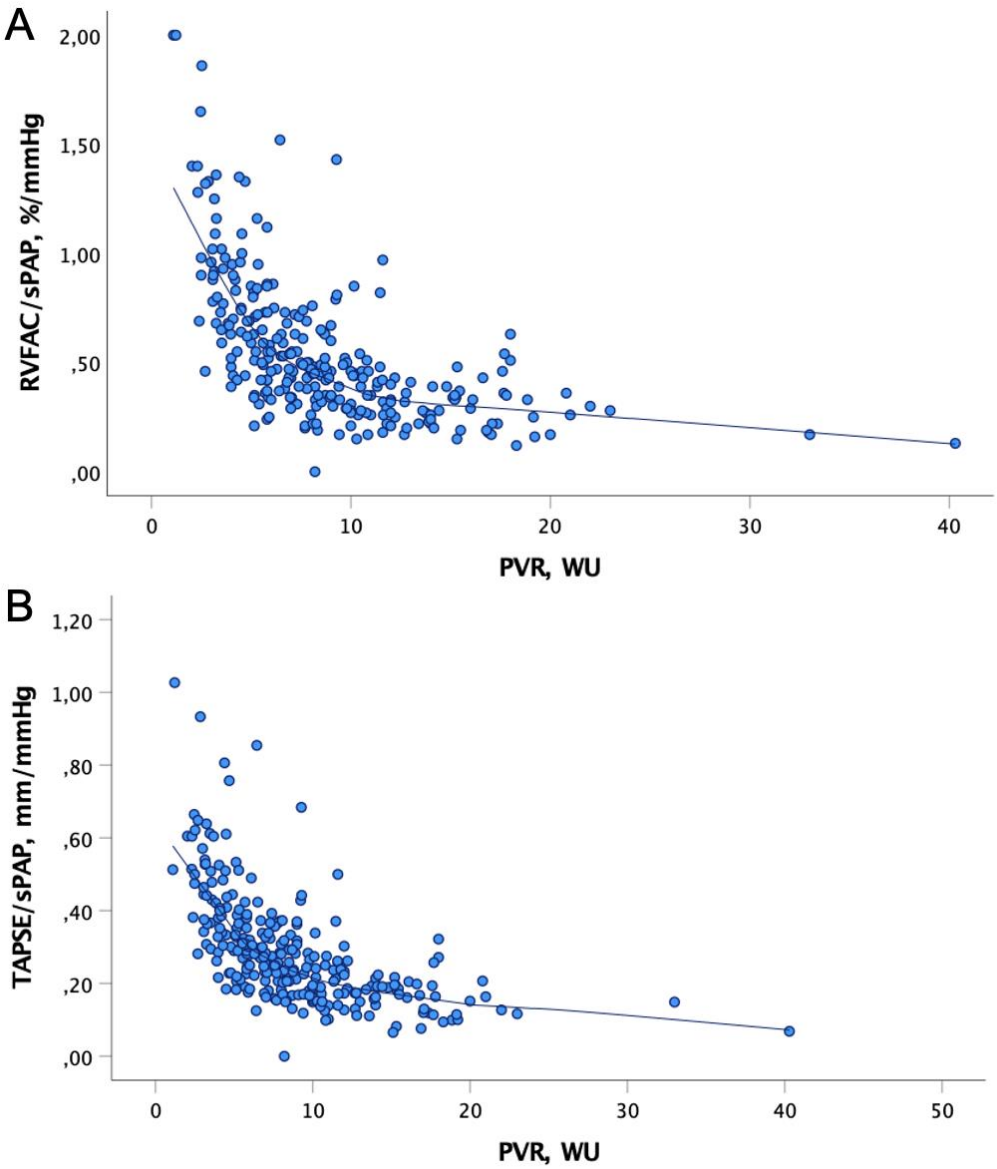

Both RVFAC/sPAP and TAPSE/sPAP showed negative correlation with PVR (respectively, r= -0.70, p<0.001, and r= -0.73, p<0.001).

Abbreviations. RVFAC: right ventricular fraction area change; TAPSE: tricuspid annular plane systolic excursion; sPAP: systolic pulmonary arterial pressure; PVR: pulmonary vascular resistance, WU: wood unit.

Figure 6. Box-and-whiskers plots showing the distribution of RVFAC according to the ESC/ERS "4-strata" (panel A) and REVEAL 2.0 (panel B).

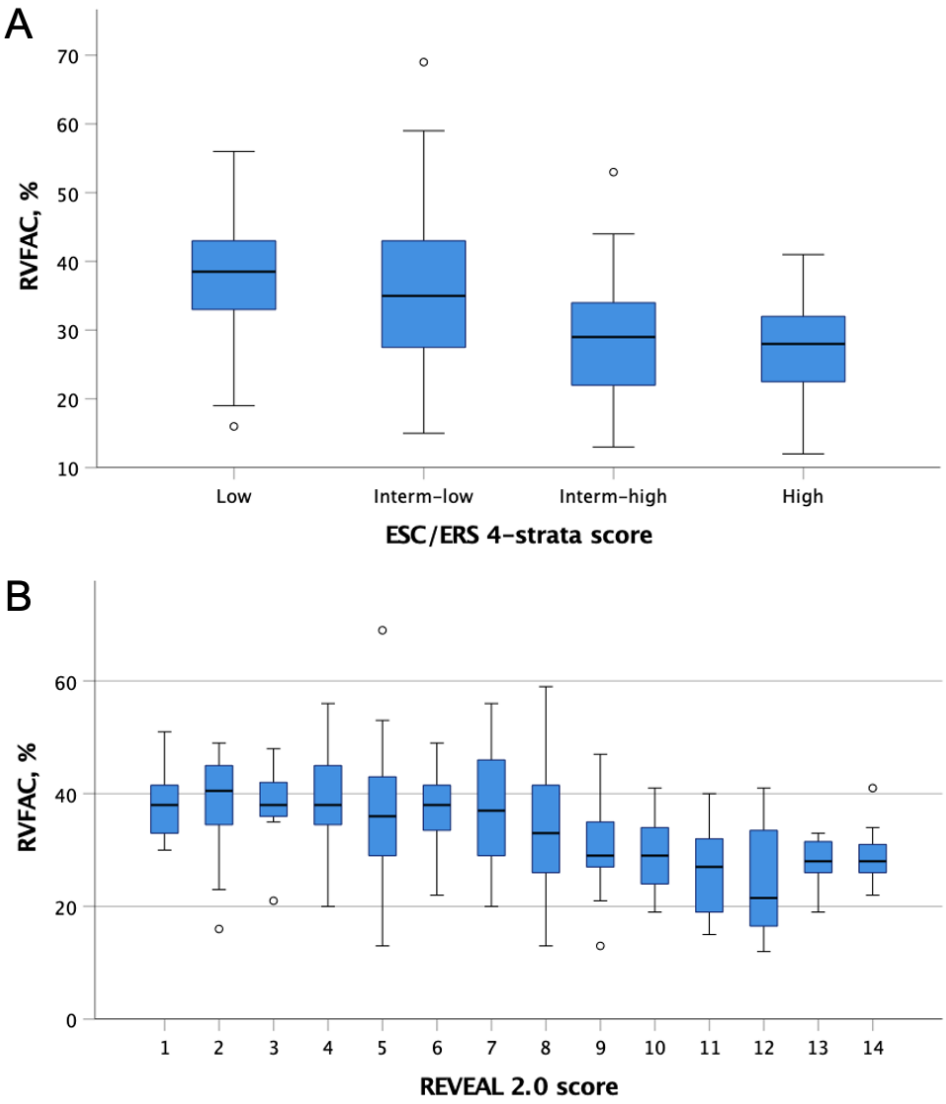

Lower RVFAC was associated with higher risk using both ESC/ERS or REVEAL 2.0 risk scores (ESC/ERS score: τ_b = -0.32, p<0.001; REVEAL 2.0 score: τ_b = -0.31, p<0.001).

Abbreviations. ESC: European Society of Cardiology; REVEAL 2.0: United States Registry to Evaluate Early and Long-Term Pulmonary Arterial Hypertension Disease Management; RVFAC: right ventricular fraction area change.

Figure 7. Box-and-whiskers plots showing the distribution of TAPSE/sPAP according to the ESC/ERS "4-strata" (panel A) and REVEAL 2.0 (panel B).

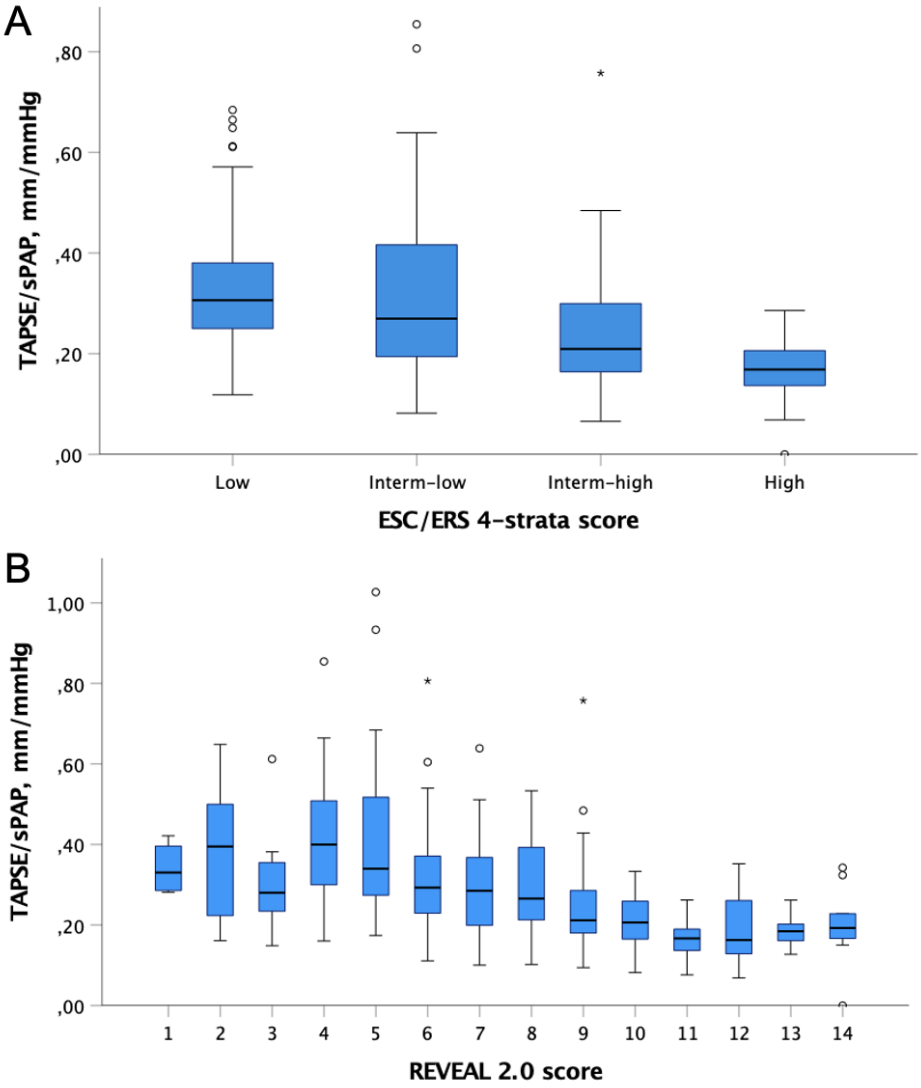

TAPSE corrected for sPAP correlated with both the ESC/ERS and REVEAL 2.0 risk scores (ESC/ERS score: τ_b = -0.30, p<0.001; REVEAL 2.0 score: τ_b = -0.35, p<0.001).

Abbreviations. ESC: European Society of Cardiology; REVEAL 2.0: United States Registry to Evaluate Early and Long-Term Pulmonary Arterial Hypertension Disease Management; TAPSE: tricuspid annular plane systolic excursion; sPAP: systolic pulmonary arterial pressure.

Figure 8. Correlation between RVEDA and global RV strain and RVFW strain.

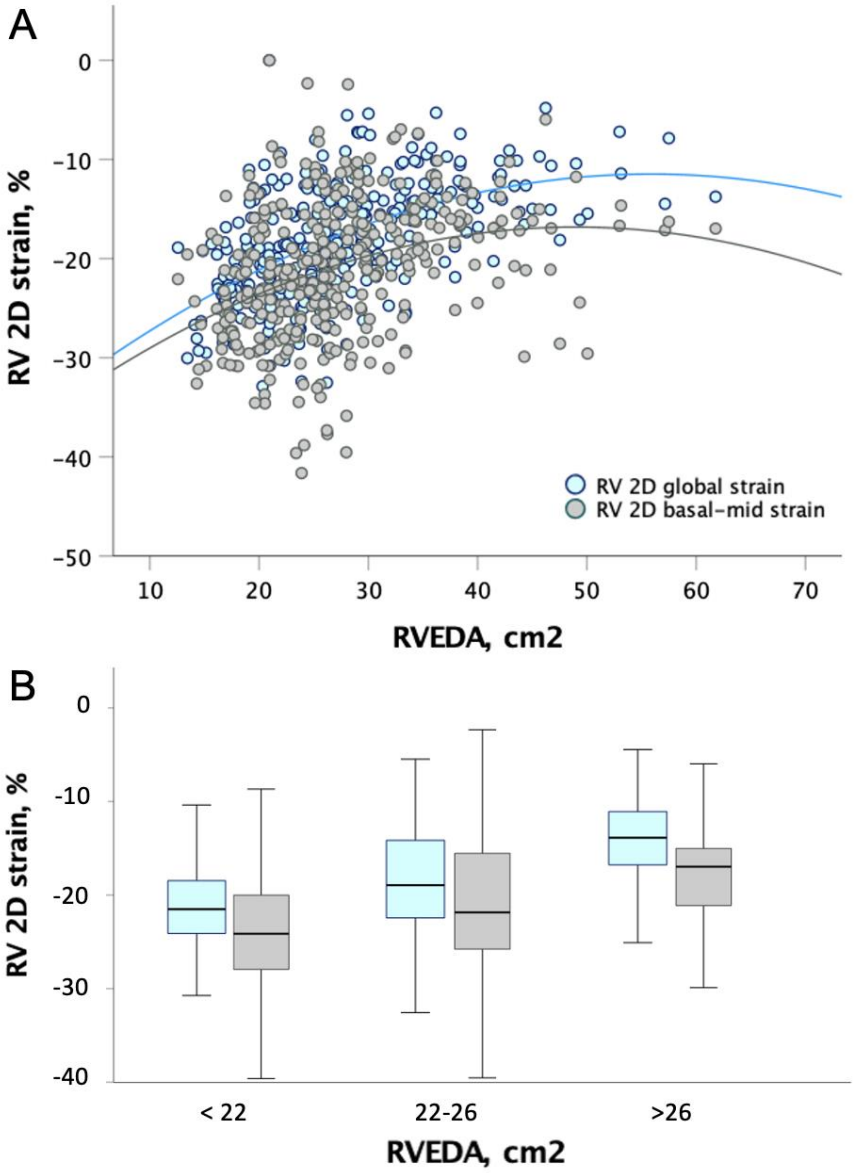

RV dilatation is associated with progressive reduction of the global RV strain and RVFW strain of the basal and middle segments. Panel A. Scatterplot of RV 2D strain versus RVEDA, based on RV global strain measurements and RVFW strain of the basal and middle segments. Panel B.

RV 2D strain median value, based on RV global strain measurements and RVFW strain of the basal and middle segments, versus tertiles of RVEDA values (< 22 cm^2; 22-26 cm^2; > 26 cm^2). Box edges represent the 25th (Q1)

and 75th (Q3) quartiles, respectively. The upper whisker is drawn at the greatest value smaller than 1.5 IQR above the third quartile, while the lower whisker is drawn at the smallest value greater than 1.5 IQR below the first quartile.

Abbreviations. RVEDA: right ventricular end-diastolic area; RV 2D strain: right ventricular two-dimensional strain; RVFW: right ventricular free wall; IQR: interquartile range.

Figure 9. Correlation between PVR and RV systolic function variables based on RV dilation.

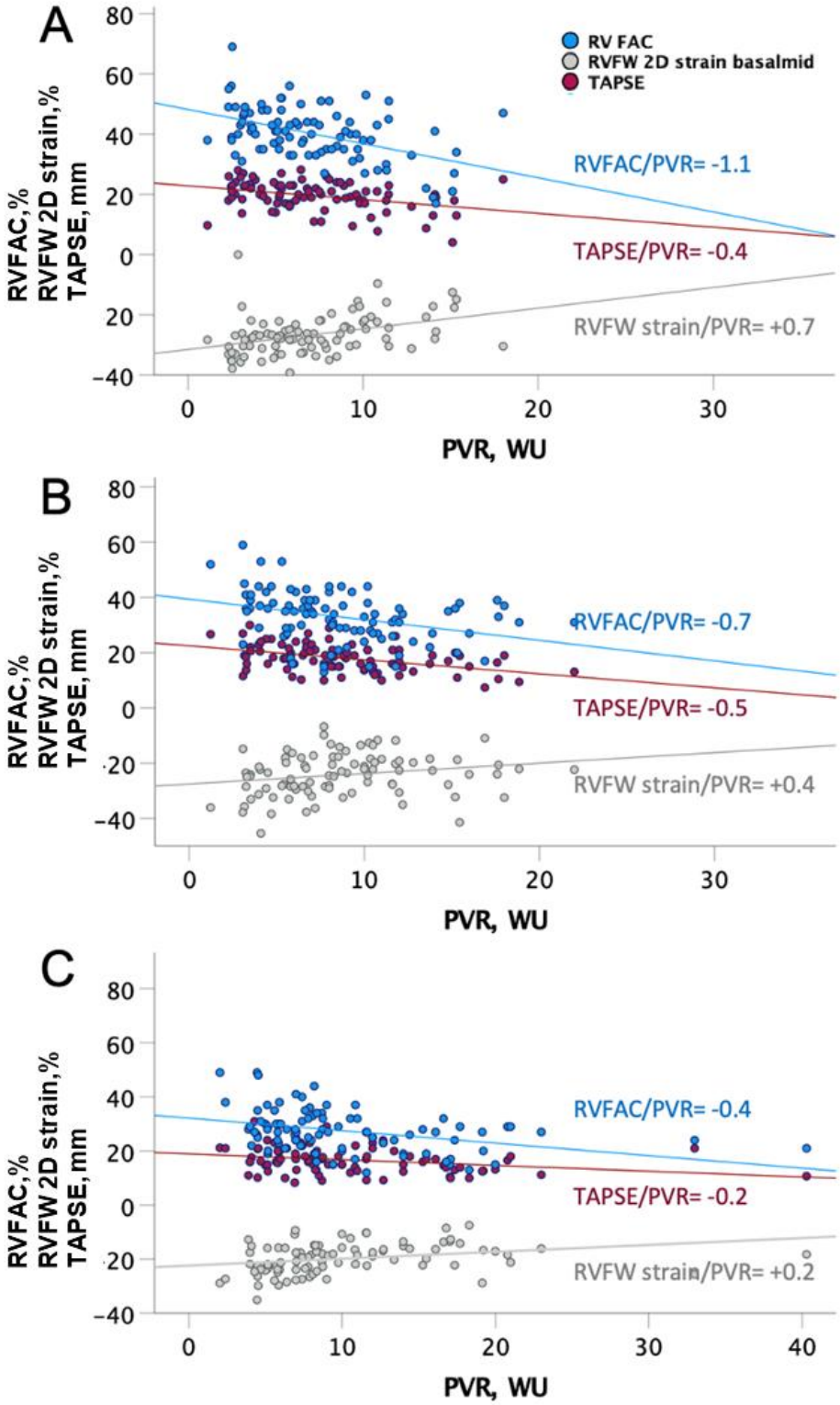

The relationship between RV systolic parameters, such as as RVFAC, RVFW strain and TAPSE, and PVR appears flattered when the RV is severely dilated. Panel A. RVFAC, RVFW strain and TAPSE, vs PVR in mildly dilated RVs (RVEDA lower tertile, 22 < cm^2) (respectively, -1.1 % per 1 PVR WU; 0.69 % per 1 PVR WU; -0.46% per 1 PVR WU, p<0.01); Panel B. RVFAC, RVFW strain and TAPSE, vs PVR in moderately dilated RVs (RVEDA intermediate tertile, 22-26 cm^2) (respectively, -0.7 % per 1 PVR WU; 0.4 % per 1 PVR WU; -0.5% per 1 PVR WU, p<0.01); Panel C. RVFAC, RVFW strain and TAPSE, vs PVR in severely dilated RVs (RVEDA higher tertile, > 26 cm^2) (respectively, -0.4 % per 1 PVR WU; 0.2 % per 1 PVR WU; -0.2% per 1 PVR WU, p<0.01).

Abbreviations. PVR: pulmonary vascular resistance, RVEDA: right ventricular end-diastolic area, RVFAC: right ventricular fraction area change, RVFW: right ventricular free wall; TAPSE: tricuspid annular plane systolic excursion, WU: wood unit.

Figure 10. Forest plot of Cox univariate analysis showing Hazard Ratios (HRs) of different echocardiographic variable for the composite endpoint of all cause mortality and hospitalization for heart failure.

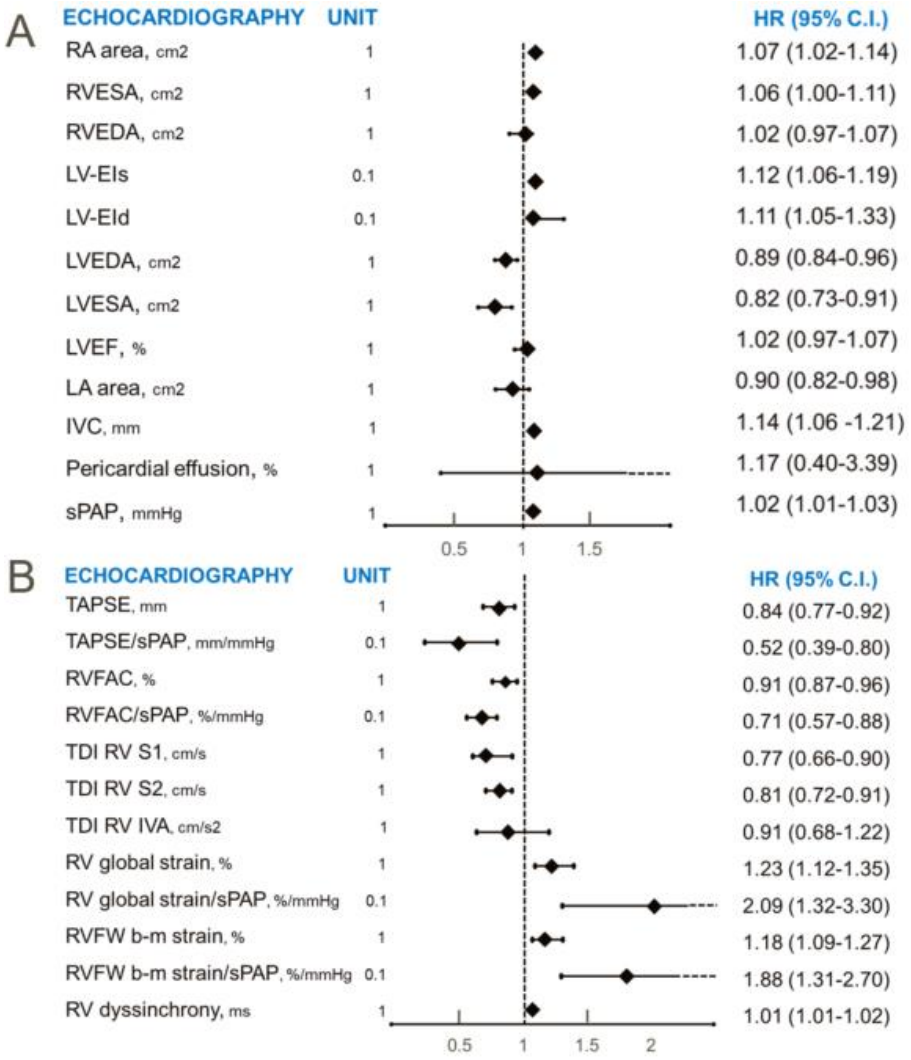

Panel A. HR for echocardiographic morphologic parameters. Panel B. HR for echocardiographic systolic functional parameters.

Abbreviations: b-m: basal-mid, EDA: end-diastolic area, EId: end-diastolic eccentricity index, EF: ejection fraction, EIs: end-systolic eccentricity index, ESA: end-systolic area, FAC: fractional area change, FW: free wall, IVC: inferior vena cava, IVA: isovolumic acceleration, S1: isovolumic velocity, LA area: left atrial area, LS: longitudinal strain, LV: left ventricle, RA area: right atrial area, RV: right ventricle, S2: systolic wave velocity, sPAP: systolic pulmonary artery pressure, TAPSE: tricuspid annular plane systolic excursion, TDI: tissue Doppler imaging.

Figure 11. Forest plot of logistic regression analysis showing the Odd Ratios (ORs) of maintaining/achieve an ESC/ERS low-risk status, based on the echocardiographic variables at baseline.

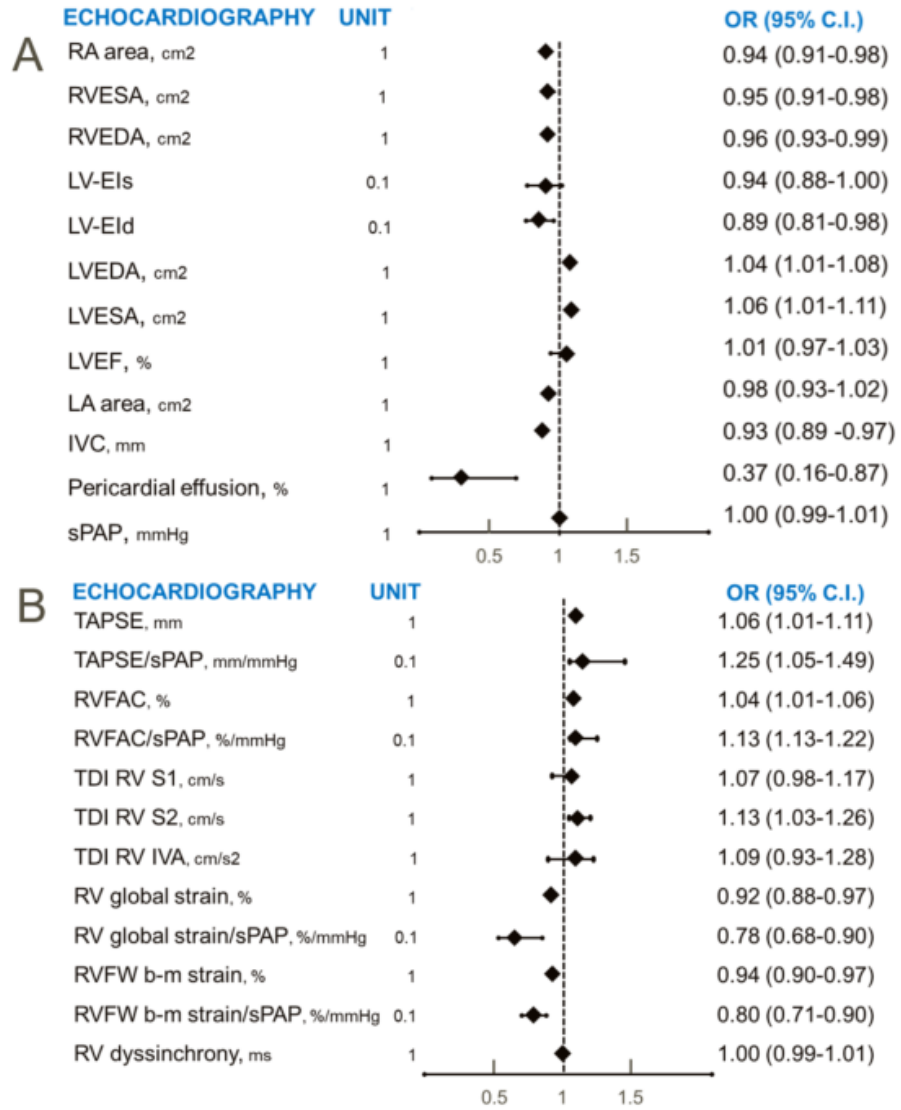

Panel A. ORs for echocardiographic morphologic parameters. Panel B. ORs for echocardiographic systolic functional parameters.

Abbreviations: b-m: basal-mid, EDA: end-diastolic area, EId: end-diastolic eccentricity index, EF: ejection fraction, EIs: end-systolic eccentricity index, ESA: end-systolic area, FAC: fractional area change, FW: free wall, IVC: inferior vena cava, IVA: isovolumic acceleration, S1: isovolumic velocity, LA area: left atrial area, LS: longitudinal strain, LV: left ventricle, RA area: right atrial area, RV: right ventricle, S2: systolic wave velocity, sPAP: systolic pulmonary artery pressure, TAPSE: tricuspid annular plane systolic excursion, TDI: tissue Doppler imaging.

Figure 12. Forest plot of logistic regression analysis showing the Odd Ratios (ORs) of maintaining/achieve a REVEAL 2.0 low-risk status (score < 6), based on the echocardiographic variables at baseline.

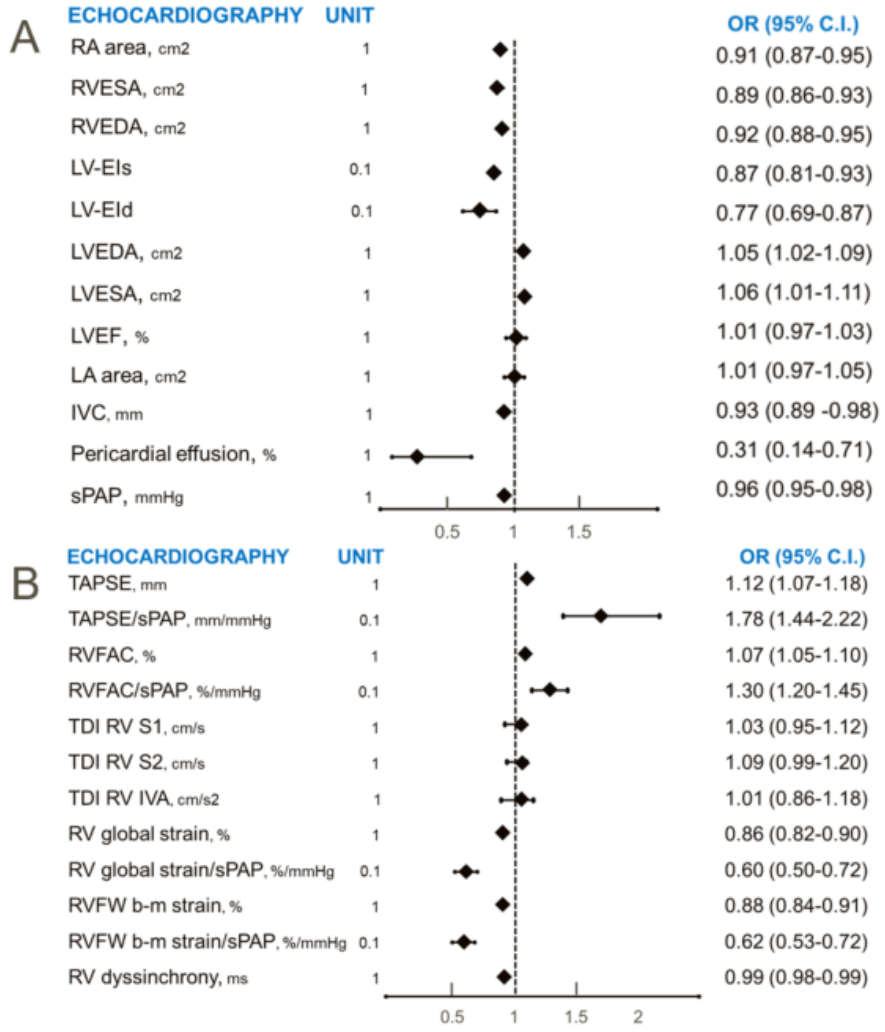

Panel A. ORs for echocardiographic morphologic parameters. Panel B. ORs for echocardiographic systolic functional parameters.

Abbreviations: b-m: basal-mid, EDA: end-diastolic area, EId: end-diastolic eccentricity index, EF: ejection fraction, EIs: end-systolic eccentricity index, ESA: end-systolic area, FAC: fractional area change, FW: free wall, IVC: inferior vena cava, IVA: isovolumic acceleration, S1: isovolumic velocity, LA area: left atrial area, LS: longitudinal strain, LV: left ventricle, RA area: right atrial area, RV: right ventricle, S2: systolic wave velocity, sPAP: systolic pulmonary artery pressure, TAPSE: tricuspid annular plane systolic excursion, TDI: tissue Doppler imaging.

Figure 13. Plot showing the impact of adding each isolated echocardiographic variable on the c-index, in case of ESC/ERS score with missing variables (i.e. WHO FC, 6MWD and BNP/NT-proBNP).

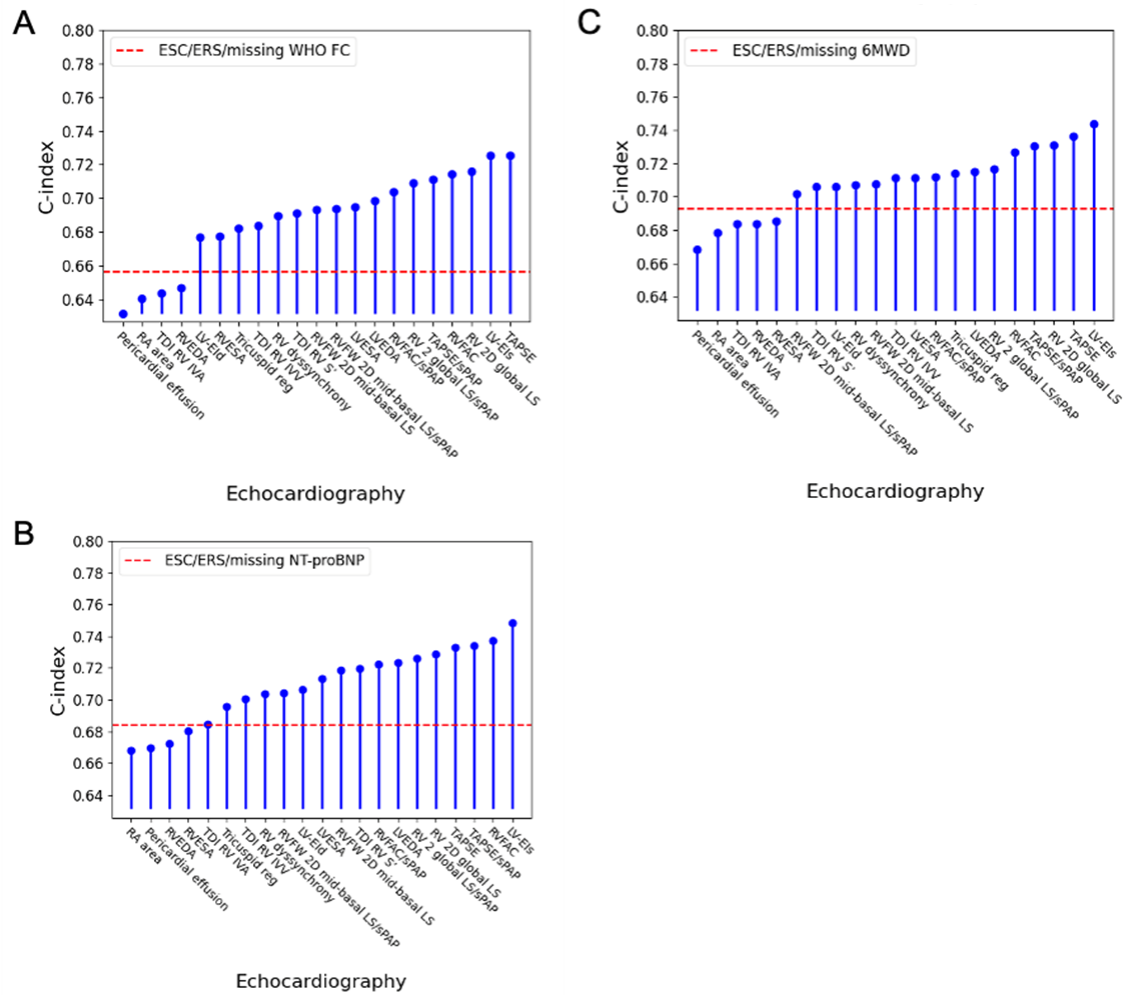

The red dot line indicate the c-index of the score with each clinical variable missing. Panel A. ESC/ERS score with WHO FC missing. Panel B. ESC/ERS score with 6MWD missing. Panel C. ESC/ERS score with BNP/NT-proBNP missing.

Abbreviations: 6MWD: six-minutes walk distance, BNP: Brain Natriuretic Peptide, b-m: basal-mid, EDA: end-diastolic area, EId: end-diastolic eccentricity index, EF: ejection fraction, EIs: end-systolic eccentricity index, ESA: end-systolic area, FAC: fractional area change, FW: free wall, IVC: inferior vena cava, IVA: isovolumic acceleration, IVV: isovolumic velocity, LA area: left atrial area, LS: longitudinal strain, LV: left ventricle, RA area: right atrial area, RV: right ventricle, S': systolic wave velocity, sPAP: systolic pulmonary artery pressure, TAPSE: tricuspid annular plane systolic excursion, TDI: tissue Doppler imaging, WHO FC: World Health Organization functional class

Figure 14. Plot showing the impact of adding each isolated echocardiographic variable on the c-index, in case of REVEAL 2.0 score with missing variables (i.e. WHO FC, 6MWD and BNP/NT-proBNP).

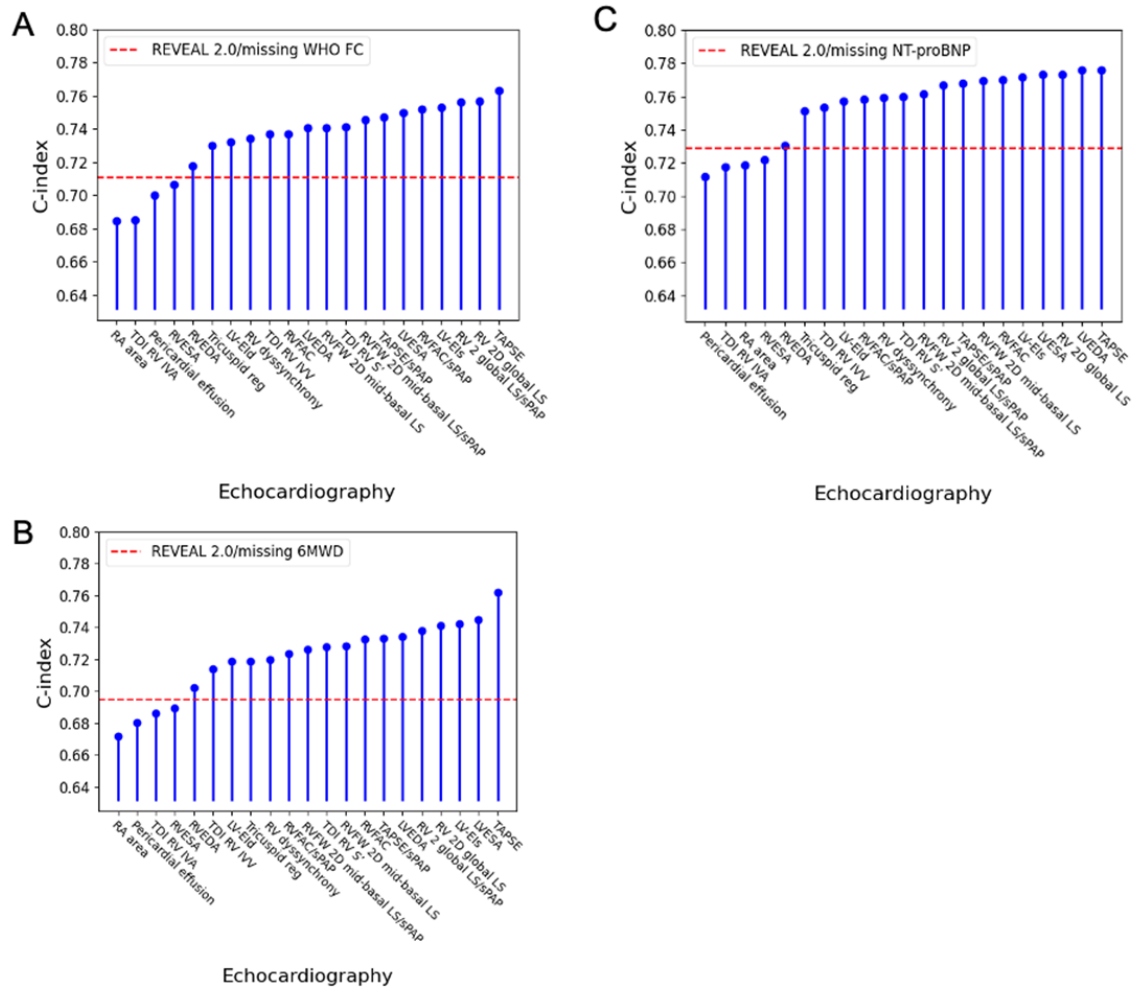

The red dot line indicate the c-index of the score with each clinical variable missing. Panel A. REVEAL 2.0 score with WHO FC missing. Panel B. REVEAL 2.0 score with 6MWD missing. Panel C. REVEAL 2.0 score with BNP/NT-proBNP missing.

Abbreviations: 6MWD: six-minutes walk distance, BNP: Brain Natriuretic Peptide, b-m: basal-mid, EDA: end-diastolic area, EId: end-diastolic eccentricity index, EF: ejection fraction, EIs: end-systolic eccentricity index, ESA: end-systolic area, FAC: fractional area change, FW: free wall, IVC: inferior vena cava, IVA: isovolumic acceleration, IVV: isovolumic velocity, LA area: left atrial area, LS: longitudinal strain, LV: left ventricle, RA area: right atrial area, RV: right ventricle, S': systolic wave velocity, sPAP: systolic pulmonary artery pressure, TAPSE: tricuspid annular plane systolic excursion, TDI: tissue Doppler imaging, WHO FC: World Health Organization functional class

Figure 15. Permutation importance analysis applied to the ESC/ERS risk model.

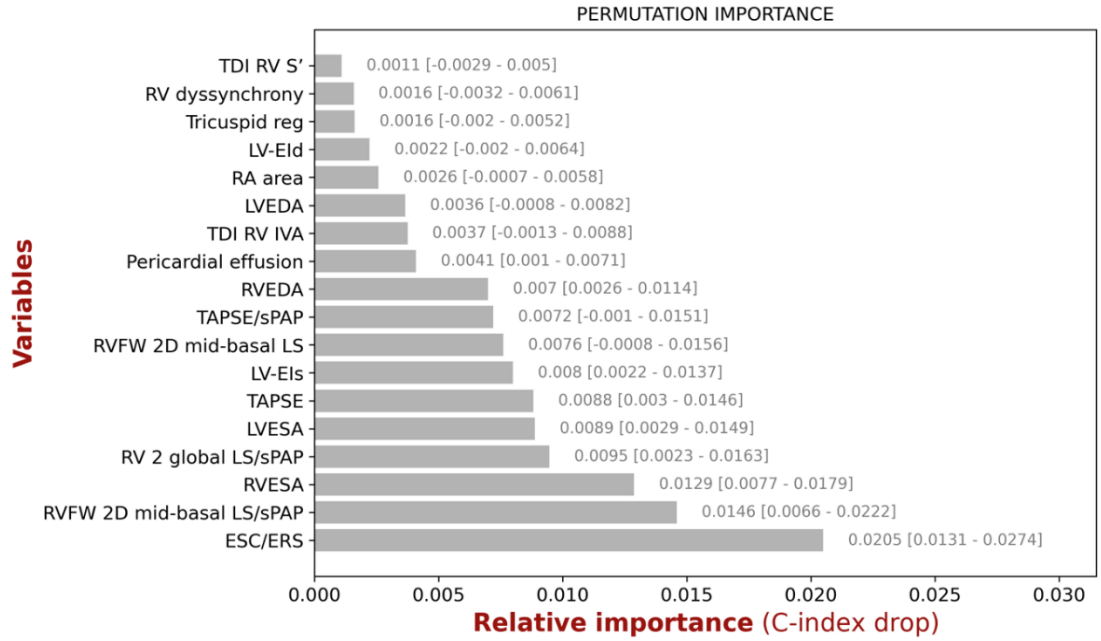

The plot shows the relative importance of echocardiographic variables when added to the ESC/ERS risk model (y-axis) by randomly shuffling their values and observing the change in the c-index (x-axis). For each variable in the model the c-index drop and the relative 95% C.I. are reported in the corresponding row.

Abbreviations: EDA: end-diastolic area, EId: end-diastolic eccentricity index, EF: ejection fraction, EIs: end-systolic eccentricity index, ESA: end-systolic area, FAC: fractional area change, FW: free wall, IVC: inferior vena cava, IVA: isovolumic acceleration, IVV: isovolumic velocity, LA area: left atrial area, LS: longitudinal strain, LV: left ventricle, RA area: right atrial area, RV: right ventricle, S': systolic wave velocity, sPAP: systolic pulmonary artery pressure, TAPSE: tricuspid annular plane systolic excursion, TDI: tissue Doppler imaging, WHO FC: World Health Organization functional class

Figure 16. Permutation importance analysis applied to the REVEAL 2.0 risk model.

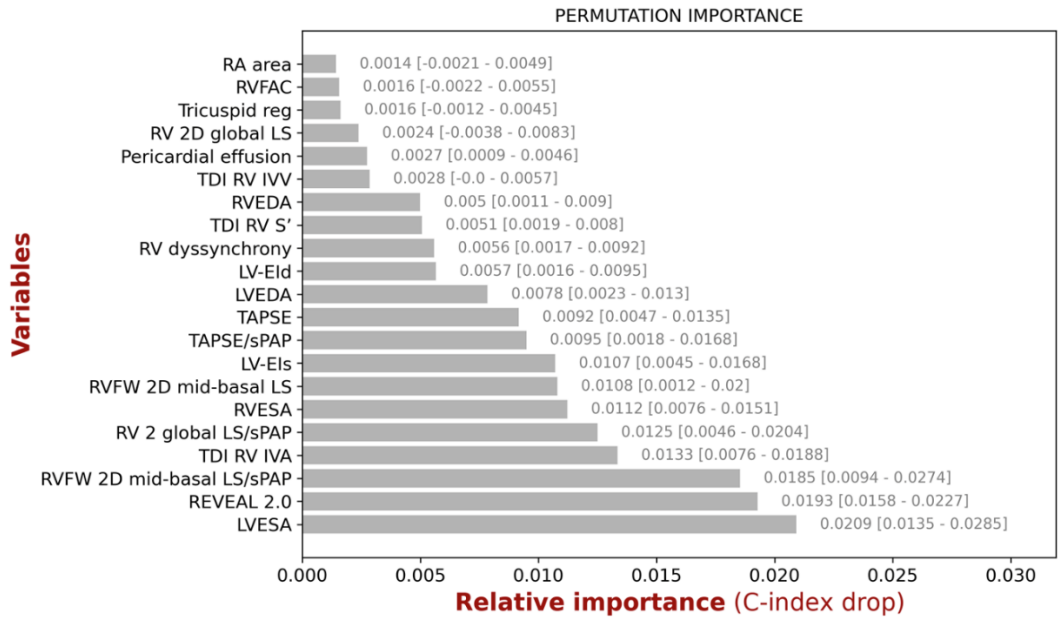

The plot shows the relative importance of echocardiographic variables when added to the REVEAL 2.0 risk model (y-axis) by randomly shuffling their values and observing the change in the c-index (x-axis). For each variable in the model the c-index drop and the relative 95% C.I. are reported in the corresponding row.

Abbreviations: EDA: end-diastolic area, EId: end-diastolic eccentricity index, EF: ejection fraction, EIs: end-systolic eccentricity index, ESA: end-systolic area, FAC: fractional area change, FW: free wall, IVC: inferior vena cava, IVA: isovolumic acceleration, IVV: isovolumic velocity, LA area: left atrial area, LS: longitudinal strain, LV: left ventricle, RA area: right atrial area, RV: right ventricle, S': systolic wave velocity, sPAP: systolic pulmonary artery pressure, TAPSE: tricuspid annular plane systolic excursion, TDI: tissue Doppler imaging, WHO FC: World Health Organization functional class

SUPPLEMENTS

Table 1. Supplementary. Correlation of echocardiographic variables with clinical and hemodynamic data, corrected for the severity of tricuspid regurgitation.

	WHO	6MWD	NTproBNP	RAP	mPAP	PVR	PA-C	CI	ESC/ERS	REVEAL
RA Area, cm2	--	--	--	--	--	--	--	--	--	--
LV-Eid, -	--	--	ρ =0.34, p= 0.03	--	ρ = 0.40, p= 0,08	ρ = 0.39, p=0.07	ρ = -0.30, p=0.07	--	--	---
LV-Eis, -	--	ρ = -0.17, p=0.08	ρ = 0.28, p=0.02	ρ = -0.24, p=0.05	ρ = 0.52, p=0.10	ρ = 0.44, p=0.05	ρ = 0.39, p=0.10	ρ = 0.17, p=0.02	--	--
RVEDA, cm2	--	r = 0.20, p=0.03	--	--	r = 0.32, p=0.02	--	--	--	--	--
RVESA, cm2	--	r = -0.27, p=0.04	--	--	r = 0.40, p=0.03	--	--	--	--	--
RVFAC,%	--									

RVFAC/sPAP, %/mmHg	--	--	--	--	--	--	--	ρ = 0.38, p=0.02	--	--
--	--	--	--	--	--	--	--	--	--	--
TAPSE/sPAP, mm/mmHg	--	--	ρ = -0.40, p=0.01	--	ρ = -0.77, p=0.01	--	ρ = 0.37, p=0.02	ρ = 0.46, p=0.02	--	--
pTDI s1' Acc slope, m/s2	--	--	--	--	--	--	--	--	--	--
pTDI s1', cm/s	--	--	--	--	--	r= -0.33, p=0.01	r= 0.30, p=0.03	r = 0.17, p=0.03		τb = -0.10, p=0.02
pTDI s2', cm/s	--	--	--	--	r= -0.26, p=0.02	--	--	--	--	--
RV 2DS global,%	--	--	--	--	--	--	--	--	--	--
RV 2DS global/sPAP, %/mmHg	--	--	--	--	ρ = 0.74, p=0.01	--	--	--	--	τb = 0.35, p= 0.01
RVFW peak 2DS mid-basal/sPAP, %/mmHg	--	--	--	--	--	--	--	--	--	--
RVFW peak 2DS mid-basal/sPAP, %/mmHg	--	--	--	--	--	--	--	ρ = 0.37, p=0.01	--	τb = 0.35, p= 0.04

RV dyssynchrony, ms	--	--	--	--	--	--	--	--	--	--
Pericardial effusion	--	--	--	--	--	--	--	--	--	--

Abbreviations: 6MWT: non-encouraged 6-minute walk test; BMI: body mass index; onset of symptoms: before diagnosis; PAH: pulmonary arterial hypertension; CI: cardiac index; CTD: connective tissue disease associated PAH; DLCO: diffusing capacity for carbon monoxide; HIV: HIV infection associated PAH; WHO: World Health Organization; BNP: brain natriuretic peptide; RAP: mean right atrial pressure; mPAP: mean pulmonary arterial pressure; CI: cardiac index; PVR: pulmonary vascular resistance; PAWP: wedge pressure; PASP: pulmonary arterial systolic pressure; RV: right ventricular end-diastolic area; LV: left ventricular end-diastolic area; TAPSE: tricupid anular plane systolic excursion; Tricuspid reg. grade: tricuspid regurgitation grade.

r = Pearson's r correlation coefficient; τ b = Kendall's tau-b correlation coefficient; ρ = Spearman rank-order correlation coefficient; d = Somers' delta correlation coefficient

Supplementary table 2. Univariate analysis of echocardiographic variables for morbi-mortality

Echocardiography		**ESC/ERS low**		**REVEAL 2.0 <7**	
	Unit	OR	p	OR	p
LVEDA, cm2	1	1.04 (1.01-1.08)	0.01	1.04 (1.01-1.09)	0.02
LVESA, cm2	1	1.06 (1.01-1.11)	0.02	1.06 (1.01-1.12)	0.03
LVEF, %	1	1.006 (0.97-1.03)	ns	1.003 (0.9-1.04)	ns
LV-EId	1	0.31 (0.12-0.83)	0.01	0.42 (0.15-1.14)	ns
LV-EIs	1	0.54 (0.29-1.01)	ns	0.68 (0.36-1.28)	ns
LA area, cm2	1	0.98 (0.93-1.02)	ns	0.99 (0.94-1.03)	ns
RVEDA, cm2	1	0.96 (0.93-0.99)	0.02	0.96 (0.93-1.01)	ns
RVESA, cm2	1	0.95 (0.91-0.98)	0.007	0.95 (0.92-0.99)	0.02
RVFAC, %	1	1.04 (1.01-1.06)	0.006	1.03 (1.01-1.05)	0.04
RVFAC/sPAP, %/mmHg	0.1	1.13 (1.13-1.22)	0.003	0.98 (0.98-1.08)	ns
TAPSE, mm	1	1.06 (1.01-1.11)	0.02	1.05 (0.99-1.11)	ns
TAPSE/sPAP, mm/mmHg	0.1	1.25 (1.05-1.49)	0.01	0.96 (0.78-1.18)	ns
TDI RV IVV, cm/s	1	1.07 (0.98-1.17)	ns	1.00 (0.90-1.10)	ns
TDI RV IVA, cm/s^2	1	1.09 (0.93-1.28)	ns	1.00 (0.83-1.21)	ns
TDI RV S', cm/s	1	1.13 (1.03-1.26)	0.01	1.12 (1.01-1.24)	0.03
RV 2D global strain, %	1	0.92 (0.88-0.97)	0.001	0.95 (0.90-0.99)	0.03
RV global strain/sPAP, %/mmHg	0.1	0.78 (0.68-0.90)	0.001	1.01 (0.85-1.20)	ns
RVFW 2D basal-mid LS, %	1	0.94 (0.90-0.97)	0.001	0.96 (0.92-0.99)	0.02
RVFW basal-mid LS/sPAP,%/mmHg	0.1	0.80 (0.71-0.90)	<0.001	0.99 (0.87-1.14)	ns
RV dyssynchrony, ms	1	1.00 (0.99-1.01)	ns	0.99 (0.95-1.09)	ns

RA area, cm2	1	0.94 (0.91-0.98)	0.003	0.94 (0.90-0.98)	0.005
TR moderate-severe, n (%)	1	0.22 (0.09-0.55)	0.001	0.24 (0.09-0.62)	0.003
IVC, mm	1	0.93 (0.88-0.97)	0.004	0.93 (0.88-0.95)	0.01
Pericardial effusion, %	1	0.37 (0.16-0.87)	0.02	0.26 (0.09-0.74)	0.01
sPAP, mmHg	1	1.001 (0.99-1.01)	ns	1.00 (0.98-1.01)	ns

2D: two dimensional, EDA: end-diastolic area, EId: end-diastolic eccentricity index, EF: ejection fraction, EIs: end-systolic eccentricity index, ESA: end-systolic area, FAC: fractional area change, FW: free wall, IVC: inferior vena cava, IVA: isovolumic acceleration, IVV: isovolumic velocity, LA area: left atrial area, LS: longitudinal strain, LV: left ventricle, RA area: right atrial area, RV: right ventricle, S': systolic wave velocity, sPAP: systolic pulmonary artery pressure, TAPSE: tricuspid annular plane systolic excursion, TDI: tissue Doppler imaging.